International Journal of Engineering Technology and Management Sciences
Website: ijetms.in Issue: 2 Volume No.7 March - April – 2023
DOI:10.46647/ijetms.2023.v07i02.052 ISSN: 2581-4621

Study Of Nanoparticle Dispersion In Capillaries Using Power Law Nanofluid Model

Rekha Bali[1], Bhawini Prasad*[2]
[1]*Professor-Department of Mathematics, Harcourt Butler Technical University, Kanpur, U.P.*
[*2]*Research Scholar-Department of Mathematics, Harcourt Butler Technical University, Kanpur, U.P.*
**Corresponding author Orcid ID: https:/orcid.org/0009-0008-7681-2052*

ABSTRACT
This paper investigates the aspects of dispersion of nanoparticles in blood capillaries linked to nanodrug delivery systems. Nanoparticles are injected intravenously in blood capillaries and the resultant fluid has been identified as nanofluid. The viscosity of nanofluid is modelled using the nanoparticle size dependent viscosity relation. The properties of blood are studied using power law fluid, owing to their physically close simulations. The dispersion model framed here has been solved applying the method used by Sankarsubramanian and Gill for deriving exchange coefficients. The study conducted gives an insight into temperature, velocity and three transport coefficients of nanoparticles dispersed in blood with respect to various parameters like heat source parameter, volume fraction, power law index, size of nanoparticles, Grashof number, Darcy number and slip parameter for small values of wall absorption parameter under steady state conditions. MATLAB software has been used to plot the graphs. The outcomes reveal that physical properties of nanoparticles like size chiefly govern their dispersion. Convergence analysis is also stated for the inhomogeneous Bessel differential equation obtained while solving the problem. The developed mathematical model has useful applications to understand the dispersion of nanodrugs in the treatment of cardio vascular diseases.
Keywords-Nanoparticle, Nanoparticle size, Nanofluid, Power-Law, Dispersion, Transport coefficient

1. Introduction

Current breakthrough in the field of nanotechnology has a profound effect on contemporary medicine because of their diverse merits. Enhanced bio-availability, greater diffusivity and controlled targeted release are some major benefits. These therapeutic nanoparticles are usually injected or inoculated into the patient's body. Blood is the first medium of contiguity as the nanoparticles enter intravenously. The study of dispersion is an important determinant to gain knowledge of the functional input requirements. The nanoparticles hit the target site only after dispersing through blood. Hence, it is exceedingly worthwhile to realize the nanoparticles dispersing in blood. This mathematical model estimates the dispersion exchange coefficients which is significant to know how much dispersion occurs.

The study of dispersion of any solute in blood has been an active domain of research. Implementing the indicator dilution method in which an amount of solute is administered in blood to comprehend the fluctuations in blood concentrations. Taylor [1] experimentally and analytically laid out the theory of dispersion of solute in steady and laminar flow through a tube. Aris [2] extended the Taylor's theory of dispersion for a steady flow manoeuvring method of moments. A more generalized dispersion model for solute dispersion in a tube for fully developed flow was given by Gill and Sankarsubramanian [3]. Gill and Sankarsubramanian [4] probed into dispersion of solute in non-uniform fully developed laminar flow. Sankarsubramanian and Gill [5] devised a new-fangled approach to investigate the dispersion by resolving the boundary value problem for unsteady convective diffusion. Sankarsubramanian and Gill [6] extended their prementioned work on dispersion taking into account interphase mass transfer through the boundary of the tube wall by

DOI:10.46647/ijetms.2023.v07i02.052 ISSN: 2581-4621

assimilating three transport coefficients. This dispersion model has substantial relevance in diffusion models for blood flow.

The dispersion theory by Taylor-Aris and dispersion model developed by Gill and Sankarsubramanian [7] has been executed by many researchers to interpret nanoparticle dispersion in various Newtonian and non-Newtonian fluids. Decuzzi et al [8] explored the diffusion of nanovectors in non-permeable as well as permeable capillaries employing Taylor's theory of dispersion. They harped upon the fact that the size of nanovector depended on the type of malignance of the tumour. Gentile et al [9] evaluated the nature of blood with nanoparticles in blood vessels modelling blood as a Casson fluid. They manifested that diffusion of nanoparticles decreased with the increase in the permeability of the vessel wall whereas vice versa results were obtained for pressure and rheological parameter. Gentile and Decuzzi [10] analysed dispersion of nanoparticles in blood vessels using Casson model with time dependency.

Shaw et al [11] presented characteristics of nanoparticle dispersion in blood flowing through a micro vessel applying two-phase flow model of blood. The core region consisting of densified red blood cells was modelled as Casson fluid and the cell free region was described using Newtonian model. Bali et al [12] analysed the dispersion of nanoparticles in blood using Herschel-Bulkley fluid in a permeable capillary. Reddy et al [13] reported nanoparticle transport in blood vessels with stenosis using couple stress fluid model. The dispersion of nanoparticles was found to be enhanced in the regions of stenosis. Bali and Gupta [14] studied nanoparticle dispersion using K-L model in micro blood vessels with stenosis and concluded that maximum diffusion occurred at the vessel wall. Surabhi et al [15] examined the transport of silver nanoparticles in blood vessels applying micro-polar fluid model. Homotopy perturbation method was used to analyse the dynamics. Reddy and Srikanth [16] studied the transport of titanium dioxide nanoparticles in blood using couple stress fluid. Rathore and Srikanth [17] analysed the transport of nanoparticles in diseased catheterized artery. These outcomes emphasis on the significance of nanodrugs for treating blockages in blood vessels.

When nanoparticles are suspended in a base fluid (in this case blood), it introduces an interaction force due to the kinematics of the new fluid formed, known as nanofluid. Choi [18] first proposed this term. Buongiaro [19] observed that the characteristics of nanofluids like dispersion was much enhanced and upgraded as compared to their base fluids. In this research analysis we have considered blood as the base fluid with nanoparticles dispersed in it, the properties of which will be described using the properties of nanofluids. The viscosity variation of nanoparticle dispersed in a base fluid, or nanofluid, was first obtained theoretically by Einstein in 1906 [20]. This model underwent modifications over time by various researchers.

Non-Newtonian nanofluids are those that do not obey Newton's law of fluids. It has been studied by many authors to describe transport of nanoparticles in base fluids. Power-law nanofluid is an example of such kind where the properties of the base fluid are characterized using power law. Santra et al [21] studied copper-water nanofluid flowing through a horizontal channel. They used power law model in describing non-Newtonian nanofluids. Hayat et al [22] also studied the power law nanofluids inculcating the effects of convective boundary conditions too. Khan and Khan [23] described the MHD flow of power law nanofluid in non-linear stretching of flat surface. The properties and importance of power law nanofluids was studied and highlighted by many researchers [24] [25].

Characterizing the size of nanoparticles dispersed in blood is important as the fundamental properties of nanoparticles are a function of their sizes [26]. Sizes define delivery of drugs stability of the nanofluid, catalytic reactivity and several other physiochemical properties. Ankamwar [27] stated the fact that selection of nanoparticles is indispensable step prior to its usage. Size of nanoparticle has potential effects in their applications. Size is the representation of surface to volume ratio which directly influences the drug loading capacity of nanoparticles in blood circulation. Nanoparticles of size around 5nm have been found to be highly effective in their performance over a controlled time interval. Ganguly and Chakraborty [28] showed the dependence of effective viscosity model for nanofluid on the diameter of the dispersed nanoparticle and their volume fraction. Pasol and

International Journal of Engineering Technology and Management Sciences
Website: ijetms.in Issue: 2 Volume No.7 March - April – 2023
DOI:10.46647/ijetms.2023.v07i02.052 ISSN: 2581-4621

Feullibois [29] gave the empirical relation of viscosity of nanofluid μ_{nf} for its viscosity dependence on their diameter and volume fraction as-

$$\mu_{nf} = \mu_f[1 + 2.5(1 - 3.4606\frac{d_{np}}{d_{bv}} + 8.6065(\frac{d_{np}}{d_{bv}})^2)\phi]$$

Where μ_f is viscosity of base fluid in which nanoparticles are dispersed, ϕ is nanoparticle volume fraction, d_{np} is diameter of the spherical shaped nanoparticles dispersed and d_{bv} is diameter of the blood vessel under consideration. Shaw [30] applied this viscosity model in drug delivery of nanoparticles in a micro vessel.
Numerous studies have proved that nanofluids hold exceptional thermophysical properties in comparison to their base fluids. Hence, it is of utmost importance to inspect the parameters that effect thermal conductivity of nanofluids. The basic model for thermal conductivity of nanofluids was devised by Maxwell [31]. This model accounted for the dispersion of spherical particles in a base fluid for considerably small volume fraction of solutes. Bruggeman [32] gave another model to discern thermal conductivity of nanofluids k_{nf} for large volume fraction of spherical nanoparticles as

$$\frac{k_{nf}}{k_f} = \frac{(3\phi - 1)\frac{k_p}{k_f} + [3(1-\phi) - 1] + \sqrt{\{(3\phi - 1)\frac{k_p}{k_f} + [(3(1-\phi) - 1]\}^2 + 8\frac{k_p}{k_f}}}{4}$$

Where k_f is thermal conductivity of base fluid in which nanoparticles are dispersed, k_p is thermal conductivity of nanoparticles and ϕ is nanoparticle volume fraction. This model has higher accuracy as it allows for the interactivity of the spherical nanoparticles as well.

The theoretical model for specific heat capacity of nanofluid was first given by Pak et al [33] for dilute solutions. An improved model for large volume fractions was given by Xuan et al [34] as

$$c_{p_{nf}} = \frac{(1-\phi)\rho_f c_{p_f} + \phi\rho_p c_{p_p}}{(1-\phi)\rho_f + \phi\rho_p}$$

Where c_{p_f} is specific heat capacity of base fluid in which nanoparticles are dispersed, c_{p_p} is specific heat capacity of nanoparticles, ρ_f is density of base fluid, ρ_p is density of nanoparticles and ϕ is nanoparticle volume fraction.

Our purpose is to investigate nanoparticle dispersion effects in blood using power law nanofluid model. Usually, the intravenous medications are therapeutic at small concentrations, but turn rather toxic at higher concentrations. Hence it is extremely important and useful to understand the role of dispersion of nanoparticles in blood. The power law nanofluid model has been employed to model the nanoparticles in blood. The equation of continuity, Navier-Stoke's equation and diffusion equation for temperature and concentration has been used for the mathematical formulation. The effects of parameters like nanoparticle size, nanoparticle volume fraction and power law index have been investigated on temperature, velocity and concentration of nanoparticles in blood. The convergence analysis for the solution of inhomogeneous Bessel's differential equation is given since the convergence of power series does not guarantee the existence of the solution. The results of this mathematical analysis will further contribute to the novel comprehension and perception of how the nanoparticles are transported in blood which will dispense revelation about the fabrication of nanoparticles in their targeted drug delivery in blood.

International Journal of Engineering Technology and Management Sciences
Website: ijetms.in Issue: 2 Volume No.7 March - April – 2023
DOI:10.46647/ijetms.2023.v07i02.052 ISSN: 2581-4621

2. Mathematical Formulation and methodology

We consider blood flow through a capillary of length L' with radius R_0 as laminar, steady and incompressible. Cylindrical co-ordinates (r', θ', z') are taken into consideration for describing the velocity of nanofluid. In the axial direction i.e., along z'-axis, u' describes the axial velocity, while v' describes the radial velocity in the capillary. The velocity along the θ'-direction is zero due to axis-symmetricity. μ_{nf} describes the viscosity of nanofluid while μ_f is viscosity of blood.

Fig.1. Geometrical representation

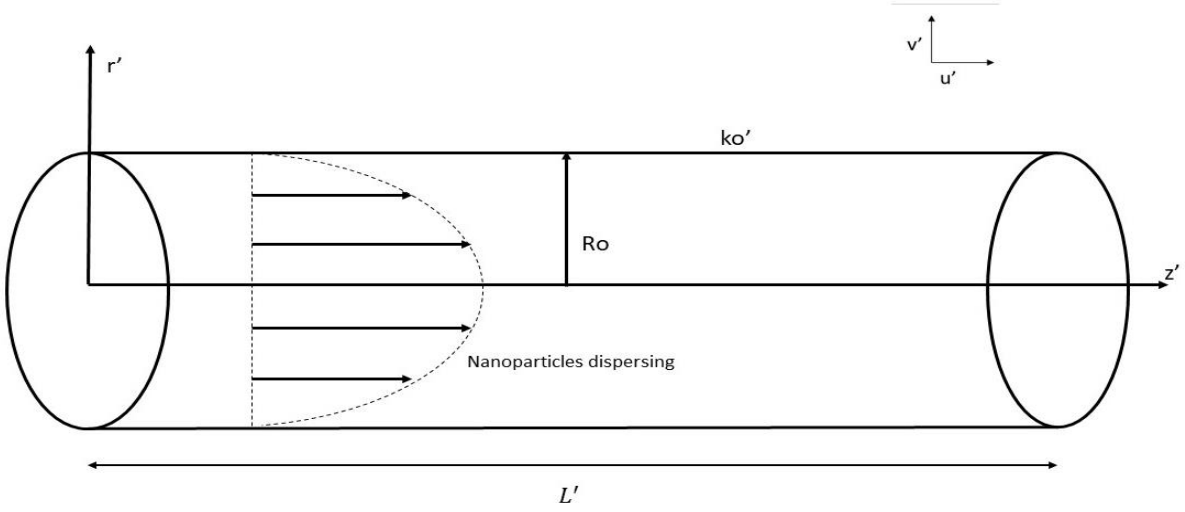

The governing equations are given as-

Equation of continuity-

$$\frac{\partial \rho_{nf}}{\partial t'} = \frac{1}{r'}\frac{\partial (r\,\rho_{nf} v')}{\partial r'} + \frac{1}{r'}\frac{\partial \rho_{nf} w'}{\partial \theta'} + \frac{\partial \rho_{nf} u'}{\partial z'} = 0 \quad (1)$$

Navier-Stokes equation-

$$\frac{\partial v'}{\partial t'} + v'\frac{\partial v'}{\partial r'} + \frac{u'}{r'}\frac{\partial v'}{\partial \theta'} - \frac{u'^2}{r'} + u'\frac{\partial v'}{\partial z'} = F_{r'} - \frac{1}{\rho_{nf}}\frac{\partial p'}{\partial r'} + \frac{\mu_{nf}}{\rho_{nf}}\left(-\frac{v'}{r^2} + \frac{1}{r'}\frac{\partial}{\partial r'}\left(r'\frac{\partial v'}{\partial r'}\right) + \frac{1}{r'^2}\frac{\partial^2 v'}{\partial \theta'^2} + \frac{\partial^2 v'}{\partial z'^2} - \frac{2}{r'^2}\frac{\partial w'}{\partial \theta'}\right) \quad (2)$$

$$\frac{\partial w'}{\partial t'} + v'\frac{\partial w'}{\partial r'} + \frac{u'}{r'}\frac{\partial w'}{\partial \theta'} - \frac{v'w'}{r'} + u'\frac{\partial w'}{\partial z'} = F_{\theta'} - \frac{1}{\rho_{nf}}\frac{\partial p'}{\partial \theta'} + \frac{\mu_{nf}}{\rho_{nf}}\left(-\frac{w'}{r^2} + \frac{1}{r'}\frac{\partial}{\partial r'}\left(r'\frac{\partial w'}{\partial r'}\right) + \frac{1}{r'^2}\frac{\partial^2 w'}{\partial \theta'^2} + \frac{\partial^2 w'}{\partial z'^2} + \frac{2}{r'^2}\frac{\partial v'}{\partial \theta'}\right) \quad (3)$$

$$\frac{\partial u'}{\partial t'} + v'\frac{\partial u'}{\partial r'} + \frac{u'}{r'}\frac{\partial u'}{\partial \theta'} + u'\frac{\partial u'}{\partial z'} = F_{z'} - \frac{1}{\rho_{nf}}\frac{\partial p'}{\partial z'} + \frac{\mu_{nf}}{\rho_{nf}}\left(\frac{1}{r'}\frac{\partial}{\partial r'}\left(r'\frac{\partial u}{\partial r'}\right) + \frac{1}{r'^2}\frac{\partial^2 u'}{\partial \theta'^2} + \frac{\partial^2 u'}{\partial z'^2}\right) \quad (4)$$

where F' in various indices stands for body forces in different co-ordinates and ρ_{nf} is density of nanofluid.

Diffusion equation for temperature of nanofluid-

$$\left(v'\frac{\partial T'}{\partial r'} + u'\frac{\partial T'}{\partial z'}\right) = \frac{k_{nf}}{\rho_{nf} c_{p_{nf}}}\left(\frac{\partial^2 T'}{\partial r'^2} + \frac{1}{r'}\frac{\partial T'}{\partial r'} + \frac{\partial^2 T'}{\partial z'^2}\right) + \frac{H}{\rho_{nf} c_{p_{nf}}} \quad (5)$$

where $c_{p_{nf}}$ is specific heat capacity of nanofluid, k_{nf} is thermal conductivity of nanofluid and ρ_{nf} is density of the nanofluid. H is constant heat generation or absorption parameter.

Diffusion equation for nanoparticles in blood-

$$\frac{1}{D'}\frac{\partial c'}{\partial t'} + u'\frac{\partial c'}{\partial z'} + v'\frac{\partial c'}{\partial r'} + w'\frac{\partial c'}{\partial \theta'} = \frac{\partial^2 c'}{\partial r'^2} + \frac{1}{r'}\frac{\partial c'}{\partial r'} + \frac{1}{r'^2}\frac{\partial^2 c'}{\partial \theta'^2} + \frac{\partial^2 c'}{\partial z'^2} + m' \quad (6)$$

where D' is diffusivity and m' is rate of increase or decrease of nanoparticles.

Nanofluids are ingenuous colloidal fluids obtained by the dispersion of 1-100nm nanoparticles in standard fluids. The treatment of viscosity variation in a nanofluid can be considered similar to the

International Journal of Engineering Technology and Management Sciences
Website: ijetms.in Issue: 2 Volume No.7 March - April – 2023
DOI:10.46647/ijetms.2023.v07i02.052 ISSN: 2581-4621

effect of in the viscosity of a solvent by adding particles of a solute. The relation of nanoparticle diameter D_p with the viscosity of nanoparticles in the nanofluid μ_{nf} applied is given as

$$\mu_{nf} = \mu_f(1 + 2.5\left(1 - 3.4606\left(\frac{D_p}{D_0}\right) + 8.6065\left(\frac{D_p}{D_0}\right)^2\right)\phi) \quad (7)$$

Where D_0 is diameter of blood capillary. μ_f is viscosity of base fluid.

The thermophysical properties largely dominate the functioning of nanoparticles in the form of nanofluids. The chief thermodynamic properties accounted for in our mathematical model are thermal conductivity and specific heat capacity. The model used for describing the thermal conductivity of nanofluid k_{nf} is given by the relation

$$\frac{k_{nf}}{k_f} = \frac{(3\phi-1)\frac{k_p}{k_f}+[3(1-\phi)-1]+\sqrt{\{(3\phi-1)\frac{k_p}{k_f}+[(3(1-\phi)-1]\}^2+8\frac{k_p}{k_f}}}{4} \quad (8)$$

Where k_f is thermal conductivity of base fluid in which nanoparticles are dispersed, k_p is thermal conductivity of nanoparticles and ϕ is nanoparticle volume fraction.

The model to determine the specific heat capacity of nanofluids $c_{p_{nf}}$ is described as

$$c_{p_{nf}} = \frac{(1-\phi)\rho_f c_{p_f}+\phi\rho_p c_{p_p}}{(1-\phi)\rho_f+\phi\rho_p} \quad (9)$$

Where c_{p_f} is specific heat capacity of base fluid in which nanoparticles are dispersed, c_{p_p} is specific heat capacity of nanoparticles, ρ_f is density of the base fluid, ρ_p is density of nanoparticles and ϕ is nanoparticle volume fraction.

The nature of base fluid of a nanofluid largely governs how the nanofluid behaves. Thus, modelling of base fluid is highly important to predict the behavior of nanofluid. Blood is the base fluid in our model, the properties of which are described by a non-Newtonian fluid called the power-law fluid. Power-law fluids reasonably describe the blood flow behavior in tubes of diameter less than 0.2 mm with shear rates less than 20 s^{-1}.
The governing equations (1) - (6) will be solved under the following assumptions:-

1. Flow is considered two dimensional.
2. Flow is steady in capillaries.
3. Flow is axisymmetric.
4. The azimuthal component of fluid velocity is zero.
5. The cross-section area is very small in capillaries; thus, the flow is described by low Reynolds number.
6. Power-law nanofluid model describes the properties of fluid in capillary.
7. A dilute solution is assumed to solve the dispersion model.
8. Free convection effects are ignored.

The modified temperature diffusion equation and Navier-Stokes equations along with their respective boundary conditions are described henceforth. The dispersion of nanoparticles in blood capillary is described later in the section under dispersion model.

The modified temperature diffusion equation followed by its boundary conditions is given as:-

$$v'\frac{\partial T'}{\partial r'} + u'\frac{\partial T'}{\partial z'} = \frac{k_{nf}}{\rho_{nf}c_{p_{nf}}}\left(\frac{\partial^2 T'}{\partial r'^2} + \frac{1}{r'}\frac{\partial T'}{\partial r'} + \frac{\partial^2 T'}{\partial z'^2}\right) \quad (10)$$

The temperature is prescribed T_0 all over surface and the temperature gradient disappears throughout the capillary axis.

International Journal of Engineering Technology and Management Sciences
Website: ijetms.in Issue: 2 Volume No.7 March - April – 2023
DOI:10.46647/ijetms.2023.v07i02.052 ISSN: 2581-4621

$\frac{\partial T\prime}{\partial r\prime} = 0$ at $r' = 0$ (11)

$T' = T_0$ at $r' = R_0$ (12)

The modified Navier-Stokes equation followed by its boundary conditions is given as:-

$-\frac{\partial p'}{\partial z'} + \frac{1}{r'}\frac{\partial}{\partial r'}(r'\tau') + g\rho_{nf}\gamma_{nf}(T' - T_0) = 0$ (13)

The shear stress is constant along the axis of the capillary because there is a constant source causing a deformation in the nanofluid, the boundary condition for is expressed as:-

τ' is finite at $r' = 0$ (14)

The shear stress relation for power law fluids is given as:-

$\tau' = -\mu_{nf}(\frac{\partial u\prime}{\partial r\prime})^{n-1}$ (15)

Where n is the power law index.

Using Darcy's law at the boundary of the capillary, we get

$u' = u'_B$ at $r' = R_0$ (16)

$\frac{\partial u\prime}{\partial r\prime} = \frac{\sigma\prime}{\sqrt{Da}}(u'_B - u'_p)$ at $r' = R_0$ (17)

where

$u'_p = -\frac{Da}{\mu_{nf}}\frac{\partial p\prime}{\partial z\prime}$ is velocity at the permeable boundary (18)

Where u'_B is slip velocity, σ' is slip parameter, Da is Darcy number.

The non-dimensional scheme is stated as:-

$r = \frac{r\prime}{R_0}$, $z = \frac{z\prime}{R_0}$, $\theta = \frac{T\prime}{T_1}$, $Gr = \frac{g\gamma_f\rho_f R_0^2 T_1}{u_{avg}\mu_f}$, $h = \frac{HR_0^2}{T_1 k_f}$, $Re = \frac{R_0 u_{avg}\rho_f}{\mu_f}$, $Da = \frac{k_f}{R_0^2}$, $u = \frac{u\prime}{u_{avg}}$, $p = \frac{R_0 p\prime}{\mu_f u_{avg}}$, $\sigma = \frac{\sigma\prime}{R_0}$ (19)

The non-dimensional equations are stated as:-

$$\frac{\partial^2\theta}{\partial r^2} + \frac{1}{r}\frac{\partial\theta}{\partial r} + h\frac{(3\phi-1)\frac{k_p}{k_f}+[3(1-\phi)-1]+\sqrt{\{(3\phi-1)\frac{k_p}{k_f}+[(3(1-\phi)-1]\}^2+8\frac{k_p}{k_f}}}{4} = 0 \quad (20)$$

$$-Re\frac{\partial p}{\partial z} = \frac{1}{r}\frac{\partial}{\partial r}\left(r\mu_f\left(1 + 2.5\left(1 - 3.4606\left(\frac{r_p}{R_0}\right) + 8.6065\left(\frac{r_p}{R_0}\right)^2\right)\phi\right)\left(\frac{\partial u}{\partial r}\right)^n\right) + \left((1-\phi) + \frac{\phi\rho_p\gamma_p}{\rho_f\gamma_f}\right)Gr\theta \quad (21)$$

The non-dimensional boundary conditions are stated as:-

$\frac{\partial\theta}{\partial r} = 0$ at $r = 0$ (22)

$\theta = 1$ at $r = 1$ (23)

International Journal of Engineering Technology and Management Sciences
Website: ijetms.in Issue: 2 Volume No.7 March - April – 2023
DOI:10.46647/ijetms.2023.v07i02.052 ISSN: 2581-4621

$$u = u_B \text{ at } r = 1 \tag{24}$$

$$\frac{\partial u}{\partial r} = \frac{\sigma}{\sqrt{Da}}(u_B - u_p) \text{ at } r = 1 \tag{25}$$

where

$$u_p = -\frac{Da}{\mu_f}\frac{\partial p}{\partial z} \text{ at } r = 1 \tag{26}$$

2.1 Solution for temperature θ

The equation (20) is solved analytically using the boundary conditions (22) and (23), and the value of θ is obtained as:-

$$\theta = \frac{h(1-r^2)((3\phi-1)\frac{k_p}{k_f}+[3(1-\phi)-1]+\sqrt{\{(3\phi-1)\frac{k_p}{k_f}+[(3(1-\phi)-1]\}^2+8\frac{k_p}{k_f}})}{4} + 1 \tag{27}$$

2.2 Solution for velocity u

The value of θ is substituted in equation (21) and is solved analytically using the boundary conditions (24) to (26) to obtain the value of u and u_B as:-

$$u = \left(\frac{h((1-\phi)+\frac{\phi\rho_p\gamma_p}{\rho_f\gamma_f})Gr\theta((3\phi-1)\frac{k_p}{k_f}+[3(1-\phi)-1]+\sqrt{\{(3\phi-1)\frac{k_p}{k_f}+[(3(1-\phi)-1]\}^2+8\frac{k_p}{k_f}})}{16\mu_f\left(1+2.5\left(1-3.4606\left(\frac{r_p}{R_0}\right)+8.6065\left(\frac{r_p}{R_0}\right)^2\right)\phi\right)}\right)^{1/n}\left(\frac{r^{\frac{3}{n}+1}}{\frac{3}{n}+1}-\frac{2r^{\frac{3}{n}-1}}{n\left(\frac{3}{n}-1\right)}\right) -$$

$$\frac{8}{nh\left((1-\phi)+\frac{\phi\rho_p\gamma_p}{\rho_f\gamma_f}\right)Gr\theta\left((3\phi-1)\frac{k_p}{k_f}+[3(1-\phi)-1]+\sqrt{\{(3\phi-1)\frac{k_p}{k_f}+[(3(1-\phi)-1]\}^2+8\frac{k_p}{k_f}}\right)}\left(\left((1-\phi)+\frac{\phi\rho_p\gamma_p}{\rho_f\gamma_f}\right)Gr\theta+\right.$$

$$\left.Re\frac{\partial p}{\partial z}\right)\left(\frac{h\left((1-\phi)+\frac{\phi\rho_p\gamma_p}{\rho_f\gamma_f}\right)Gr\theta\left((3\phi-1)\frac{k_p}{k_f}+[3(1-\phi)-1]+\sqrt{\{(3\phi-1)\frac{k_p}{k_f}+[(3(1-\phi)-1]\}^2+8\frac{k_p}{k_f}}\right)}{16\mu_f\left(1+2.5\left(1-3.4606\left(\frac{r_p}{R_0}\right)+8.6065\left(\frac{r_p}{R_0}\right)^2\right)\phi\right)}\right)^{\frac{1}{n}}\left(\frac{r^{\frac{3}{n}-1}}{\frac{3}{n}-1}-\right.$$

$$\left.\frac{2r^{\frac{3}{n}+1}}{\left(\frac{1}{n}-1\right)\left(\frac{3}{n}+1\right)}\right)+\frac{8}{nh\left((1-\phi)+\frac{\phi\rho_p\gamma_p}{\rho_f\gamma_f}\right)Gr\theta\left((3\phi-1)\frac{k_p}{k_f}+[3(1-\phi)-1]+\sqrt{\{(3\phi-1)\frac{k_p}{k_f}+[(3(1-\phi)-1]\}^2+8\frac{k_p}{k_f}}\right)}\left(\left((1-\phi)+\right.\right.$$

$$\left.\left.\frac{\phi\rho_p\gamma_p}{\rho_f\gamma_f}\right)Gr\theta+\right.$$

$$\left.Re\frac{\partial p}{\partial z}\right)\left(\frac{h\left((1-\phi)+\frac{\phi\rho_p\gamma_p}{\rho_f\gamma_f}\right)Gr\theta\left((3\phi-1)\frac{k_p}{k_f}+[3(1-\phi)-1]+\sqrt{\{(3\phi-1)\frac{k_p}{k_f}+[(3(1-\phi)-1]\}^2+8\frac{k_p}{k_f}}\right)}{16\mu_f\left(1+2.5\left(1-3.4606\left(\frac{r_p}{R_0}\right)+8.6065\left(\frac{r_p}{R_0}\right)^2\right)\phi\right)}\right)^{\frac{1}{n}}\left(\frac{4n-9n^2+n^3}{(9-n^2)(1-n)}\right)-$$

International Journal of Engineering Technology and Management Sciences
Website: ijetms.in Issue: 2 Volume No.7 March - April – 2023
DOI:10.46647/ijetms.2023.v07i02.052 ISSN: 2581-4621

$$\left(\frac{h\left((1-\phi)+\frac{\phi\rho_p\gamma_p}{\rho_f\gamma_f}\right)Gr\theta\left((3\phi-1)\frac{k_p}{k_f}+[3(1-\phi)-1]+\sqrt{\{(3\phi-1)\frac{k_p}{k_f}+[(3(1-\phi)-1]\}^2+8\frac{k_p}{k_f}}\right)}{16\mu_f\left(1+2.5\left(1-3.4606\left(\frac{r_p}{R_0}\right)+8.6065\left(\frac{r_p}{R_0}\right)^2\right)\phi\right)}\right)^{\frac{1}{n}}\left(\frac{n-n^2-6}{9-n^2}\right)+u_B$$

(28)

Applying boundary condition (25) and (26) to find the value of u_B
At $r=1$ in
$\frac{\partial u}{\partial r}=$

$$\left(\frac{1}{\mu_f\left(1+2.5\left(1-3.4606\left(\frac{r_p}{R_0}\right)+8.6065\left(\frac{r_p}{R_0}\right)^2\right)\phi\right)}\right)^{1/n}\left(\frac{h\left((1-\phi)+\frac{\phi\rho_p\gamma_p}{\rho_f\gamma_f}\right)Gr\theta\left((3\phi-1)\frac{k_p}{k_f}+[3(1-\phi)-1]+\sqrt{\{(3\phi-1)\frac{k_p}{k_f}+[(3(1-\phi)-1]\}^2+8\frac{k_p}{k_f}}\right)}{4}\left(\frac{1}{2}\right)-\frac{\left((1-\phi)+\frac{\phi\rho_p\gamma_p}{\rho_f\gamma_f}\right)Gr\theta}{2}-\frac{Re}{2}\frac{\partial p}{\partial z}\right)^{1/n}$$

(29)

$\therefore$

$$\left(\frac{1}{\mu_f\left(1+2.5\left(1-3.4606\left(\frac{r_p}{R_0}\right)+8.6065\left(\frac{r_p}{R_0}\right)^2\right)\phi\right)}\right)^{1/n}\left(\frac{h\left((1-\phi)+\frac{\phi\rho_p\gamma_p}{\rho_f\gamma_f}\right)Gr\theta\left((3\phi-1)\frac{k_p}{k_f}+[3(1-\phi)-1]+\sqrt{\{(3\phi-1)\frac{k_p}{k_f}+[(3(1-\phi)-1]\}^2+8\frac{k_p}{k_f}}\right)}{4}\left(\frac{\left((1-\phi)+\frac{\phi\rho_p\gamma_p}{\rho_f\gamma_f}\right)Gr\theta}{2}-\frac{Re}{2}\frac{\partial p}{\partial z}\right)^{1/n}=\frac{\sigma}{\sqrt{Da}}\left(u_B+\frac{Da}{\mu_f}\frac{\partial p}{\partial z}\right) \quad (30)$$

We get u_B as

$u_B=$

$$\frac{\sqrt{Da}}{\sigma}\left(\frac{1}{\mu_f\left(1+2.5\left(1-3.4606\left(\frac{r_p}{R_0}\right)+8.6065\left(\frac{r_p}{R_0}\right)^2\right)\phi\right)}\right)^{1/n}\left(\frac{h\left((1-\phi)+\frac{\phi\rho_p\gamma_p}{\rho_f\gamma_f}\right)Gr\theta\left((3\phi-1)\frac{k_p}{k_f}+[3(1-\phi)-1]+\sqrt{\{(3\phi-1)\frac{k_p}{k_f}+[(3(1-\phi)-1]\}^2+8\frac{k_p}{k_f}}\right)}{4}\left(\frac{\left((1-\phi)+\frac{\phi\rho_p\gamma_p}{\rho_f\gamma_f}\right)Gr\theta}{2}-\frac{Re}{2}\frac{\partial p}{\partial z}\right)^{1/n}-\frac{Da}{\mu_f}\frac{\partial p}{\partial z} \quad (31)$$

2.3 Dispersion model

The modified diffusion equation (5) using the assumptions and the boundary conditions are given as

$$\frac{\partial c'}{\partial t'}+u'\frac{\partial c'}{\partial z'}=D_m\left(\frac{1}{r'}\frac{\partial}{\partial r'}\left(r'\frac{\partial c'}{\partial r'}\right)+\frac{\partial^2 c'}{\partial z'^2}\right) \quad (32)$$

Where t'denotes the time in dimensional form.

The nanoparticles are distributed uniformly in the capillary at $z'=0$ therefore the initial concentration distribution is described as

$$c'(0,z',r')=\omega'(z')\xi'(r') \quad (33)$$

International Journal of Engineering Technology and Management Sciences
Website: ijetms.in Issue: 2 Volume No.7 March - April – 2023
DOI:10.46647/ijetms.2023.v07i02.052 ISSN: 2581-4621

Where $\omega'(z') = \frac{R_0\delta(z')}{d'^2}$, $\delta(z')$ is the Dirac Delta function (34)

And $\xi'(r') = \begin{cases} 1 & 0 < r' \leq d' \\ 0 & d' < r' \leq R_0 \end{cases}$ (35)

Where d' is the initial distribution.

Initially, at the beginning of the dispersion process

$c'(t', z', r') = finite\ at\ r' = 0$ (36)

Diffusion of nanoparticles at the capillary wall can be expressed as

$-D_m \frac{\partial c'(t',z',r')}{\partial r'} = k_0' c'(t', z', r')$ at $r' = R_0$ (37)

Where k_0' is the permeability at the capillary wall

The expression for finite quantity of nanoparticles in the blood stream at any instant of time is

$c'(t'z', r') = \frac{\partial c\prime(t',z',r')}{\partial z\prime} = 0$ at $z' = \infty$ (38)

The non-dimensional scheme is stated as:-

$t = \frac{D_m t\prime}{R_0^2}, Pe = \frac{R_0 u_{avg}}{D_m}, c = \frac{c\prime}{c_0}, \beta = \frac{k\prime_0 R_0}{D_m}, u = \frac{u\prime}{u_{avg}}, r = \frac{r\prime}{R_0}, z = \frac{z\prime}{R_0}$ (39)

Where is Pe Peclet number, c_0 is reference concentration and β is non-dimensional wall absorption parameter.

The non-dimensional equation is written as

$\frac{\partial c}{\partial t} + u\frac{\partial c}{\partial z} = \frac{1}{r}\frac{\partial}{\partial r}\left(r\frac{\partial c}{\partial r}\right) + \frac{1}{Pe^2}\frac{\partial^2 c}{\partial z^2}$ (40)

The non-dimensional initial and boundary conditions are given as

$c = \omega(z)\xi(r)$ where $\omega(z) = \frac{\delta(z)}{d^2 Pe}$ (41)

And $\xi(r) = \begin{cases} 1 & 0 < r \leq d \\ 0 & d \leq r \leq 1 \end{cases}$

$c = finite\ at\ r = 0$ (42)

$\frac{\partial c}{\partial r} = -\beta c\ at\ r = 1$ (43)

$c = \frac{\partial c}{\partial z} = 0$ at $z = \infty$ (44)

2.3.1 Solution of the dispersion model

The solution of convective diffusion equation in non-dimensional form is given using the method adopted by Sankarsubramanian and Gill [6] as

$c = \sum_{i=0}^{\infty} \psi_i \frac{\partial c_m}{\partial z^i}$ (45)

where the non-dimensional mean concentration c_m is described as $c_m = 2\int_0^1 cr\ dr$ and $\psi_i(t, r), i = 0,1,2, \ldots$ is a function of time and radial distance. (46)

The governing equation (40) is multiplied by $2r$ and integrated with respect to r from 0 to 1

International Journal of Engineering Technology and Management Sciences
Website: ijetms.in Issue: 2 Volume No.7 March - April – 2023
DOI:10.46647/ijetms.2023.v07i02.052 ISSN: 2581-4621

$$\frac{\partial c_m}{\partial t} = \frac{1}{Pe^2}\frac{\partial^2 c_m}{\partial z^2} + 2\frac{\partial c}{\partial r}\Big|_{r=1} - 2\frac{\partial}{\partial z}\int_0^1 ucr\, dr \quad (47)$$

The dispersion model for c_m with time dependent exchange coefficient using equation (45) in equation (47)

$$\frac{\partial c_m}{\partial t} = \sum_{i=0}^{\infty} K_i \frac{\partial^i c_m}{\partial z^i} \quad (48)$$

Where

$$K_i = \frac{\delta_{i2}}{Pe^2} + 2\frac{\partial \psi_i}{\partial r}\Big|_{r=1} - 2\int_0^1 \psi_{i-1}\, ur\, dr\ ,\ i = 0,1,2,\ldots\ldots,\ \ \psi_{-1} = 0 \quad (49)$$

Here $\delta_{ij} = \begin{cases} 1 & i = j \\ 0 & i \neq j \end{cases}$ (50)

The resultant dispersion model for mean concentration is given as

$$\frac{\partial c_m}{\partial t} = K_0 c_m + K_1 \frac{\partial c_m}{\partial z} + K_2 \frac{\partial^2 c_m}{\partial z^2} \quad (51)$$

Where

$$K_i = \frac{\delta_{i2}}{Pe^2} + 2\frac{\partial \psi_i}{\partial r}\Big|_{r=1} - 2\int_0^1 \psi_{i-1}\, ur\, dr\ ,\ i = 0,1,2 \quad (52)$$

The exchange coefficient K_0 is due to non-zero nanoparticle flux at the capillary wall, K_1 exists due to the convection coefficient because of the velocity of nanoparticle and K_2 is the dispersion coefficient due to molecular diffusion and velocity of nanofluid. The terms K_i for $i = 3,4,5,\ldots..$ have been neglected as the contribution of higher order terms is insignificant.

The nanoparticle concentration is thus expressed as

$$c = \sum_{i=0}^{2} \psi_i \frac{\partial^i c_m}{\partial z^i} \quad (53)$$

For solving equation (51) and (52), we need to find the boundary conditions. Using equation (45) in equation (40). Equating the coefficients of $\frac{\partial^l c_m}{\partial z^l}$ for $l = 0,1,2$ and obtaining

$$\frac{\partial \psi_i}{\partial t} = \frac{1}{r}\frac{\partial}{\partial r}\left(r\frac{\partial \psi_i}{\partial r}\right) - u\psi_{l-1} + \frac{1}{Pe^2}\psi_{l-2} - \sum_{i=0}^{l} K_i \psi_{l-i} \quad \text{where } l = 0,1,2 \quad (54)$$

and $\psi_{-1} = \psi_{-2} = 0$ (55)

The initial and boundary conditions are obtained from (41) to (44), described as

$$c_m = 2\omega\int_0^1 \xi r\, dr \text{ at } t = 0 \quad (56)$$

$$\psi_0 = \frac{\xi}{2\int_0^1 \xi r\, dr} \text{ at } t = 0 \quad (57)$$

$$\psi_l = 0, l = 1,2 \text{ at } t = 0 \quad (58)$$

$$\frac{\partial \psi_l}{\partial r} = 0, l = 0,1,2 \text{ at } r = 0 \quad (59)$$

$$\frac{\partial \psi_l}{\partial r} = -\beta\psi_l, l = 0,1,2 \text{ at } r = 1 \quad (60)$$

$$c_m = \frac{\partial c_m}{\partial z} = 0 \text{ at } z = \infty \quad (61)$$

Using condition (55) in (52), we have an additional condition as

$$\int_0^1 \psi_l\, r\, dr = \frac{1}{2}\delta_{l0} \text{ for } l = 0,1,2 \quad (62)$$

International Journal of Engineering Technology and Management Sciences
Website: ijetms.in Issue: 2 Volume No.7 March - April – 2023
DOI:10.46647/ijetms.2023.v07i02.052 ISSN: 2581-4621

Where δ_{l0} is defined by (50)

2.3.1.1 Solution for ψ_0 and K_0

The value of ψ_0 and K_0 are independent of velocity of nanofluid, thus they can be obtained directly using the boundary conditions (55)

$$\frac{\partial \psi_0}{\partial t} = \frac{1}{r}\frac{\partial}{\partial r}\left(r\frac{\partial \psi_0}{\partial r}\right) - K_0\psi_0 \quad (63)$$

With an additional condition on ψ_0 as $\int_0^1 \psi_0\, r\, dr = 1/2$ (64)

The solution on non-homogeneous boundary value problem (63) using Bessel equation satisfying the conditions (56)-(62) and (64) is given as

Let $\psi_0(t,r) = e^{\{-\int_0^t K_0(\eta)d\eta\}}\varrho(t,r)$ (65)

Using this transformation (65), we get an equation in terms of $\varrho(t,r)$ that has to satisfy

$$\frac{\partial \varrho}{\partial t} = \frac{1}{r}\frac{\partial}{\partial r} r\frac{\partial \varrho}{\partial r} \quad (66)$$

$$\varrho(0,r) = \psi_0(0,r) = \frac{\xi(r)}{2\int_0^1 r\xi(r)dr} \quad (67)$$

$$\frac{\partial \varrho}{\partial r}(t,1) = -\beta\varrho(t,1) \quad (68)$$

$$\varrho(t,0) = finite \quad (69)$$

Let the solution be of the form

$$\varrho(t,r) = \sum_{m=0}^{\infty} A_m e^{-\lambda_m^2 t} \quad (70)$$

Using the well-known [35] identity

$$(\frac{\partial \varrho}{\partial t})_r(\frac{\partial r}{\partial \varrho})_t = -(\frac{\partial r}{\partial t})_\varrho \quad (71)$$

We convert (66) into (72) as

$$-\frac{1}{2}\frac{\partial r^2}{\partial t} = \frac{\partial}{\partial \varrho}(r\frac{\partial \varrho}{\partial r}) \quad (72)$$

Integrating it with respect to ϱ yields

$$-\frac{1}{2}\frac{\partial}{\partial t}\int_{\varrho_0}^{\varrho} r^2 d\varrho = (r\frac{\partial \varrho}{\partial r}) \quad (73)$$

By substituting (70) into (73), we obtain the solution for $\varrho(t,r)$ by equating the coefficients on each side. Thus, the solution of (66) to (69) is given as

$$\varrho(t,r) = \sum_{m=0}^{\infty} A_m J_0(\lambda_m r) e^{-\lambda_m^2 t} \quad (74)$$

Now, using (65), we get

$$\psi_0 = \frac{\sum_{m=0}^{\infty} A_m J_0(\lambda_m r) e^{-\lambda_m^2 t}}{2\sum_{m=0}^{\infty}(\frac{A_m}{\lambda_m}) J_1(\lambda_m) e^{-\lambda_m^2 t}}$$ where J_0 and J_1 are Bessel functions (75)

and λ_m are the roots of Bessel equation

$$\lambda_m J_1(\lambda_m) = \beta J_0(\lambda_m)\,, m = 0,1,2,\ldots.. \quad (76)$$

Also $A_m = \frac{\lambda_m^2 \int_0^1 r\xi J_0(\lambda_m r)dr}{(\lambda_m^2+\beta^2)J_0^2(\lambda_m)\int_0^1 r\xi\, dr}, m = 0,1,2,\ldots..$ (77)

International Journal of Engineering Technology and Management Sciences
Website: ijetms.in Issue: 2 Volume No.7 March - April – 2023
DOI:10.46647/ijetms.2023.v07i02.052 ISSN: 2581-4621

K_0 is obtained from the initial condition as

$$K_0 = 2\frac{\partial \psi_0}{\partial r}\Big|_{r=1} = -\frac{\sum_{m=0}^{\infty} A_m \lambda_m J_1(\lambda_m) e^{-\lambda_m^2 t}}{\sum_{m=0}^{\infty} (\frac{A_m}{\lambda_m}) J_1(\lambda_m) e^{-\lambda_m^2 t}} \quad (78)$$

For steady state, $t \to \infty$, thus, equations (49) and (65) give the undermentioned asymptotic representation for the function ψ_0 and K_0

$$\lim_{t\to\infty} \psi_0 = \frac{\lambda_0}{2J_1(\lambda_0)} J_0(\lambda_0 r) \text{ and } \lim_{t\to\infty} K_0 = -\lambda_0^2 \quad (79)$$

where λ_0 is the smallest root of the Bessel's equation (76)

2.3.1.2 Solution for K_i and ψ_i , i=1,2

Under steady flow conditions, the value of K_i , i=1,2 is derived applying the value of nanofluid velocity obtained using power-law nanofluid model. The function ψ_i, i=1,2 for steady state condition is found as

$$\frac{1}{r}\frac{\partial}{\partial r}\left(r\frac{\partial \psi_l}{\partial r}\right) + \lambda_0^2 \psi_l = u\psi_{l-1} - \frac{1}{Pe^2}\psi_{l-2} + \sum_{i=1}^{l} K_i \psi_{l-i} + K_l \psi_0 \quad \text{where } l=1,2 \text{ and } \psi_{-1}0 \quad (80)$$

For steady state K_i , i=1,2 reduce to

$$K_l = \frac{\delta_{l2}}{Pe^2} + 2\frac{\partial \psi_i}{\partial r}\Big|_{r=1} - 2\int_0^1 ru\psi_{l-1}\, dr \quad , \quad l = 1,2 \quad (81)$$

The boundary conditions on $\psi_l,\ l = 1,2$

$$\psi_l = finite \text{ or } \frac{\partial \psi_l}{\partial r} = 0 \text{ at } r = 0,\ l = 1,2 \quad (82)$$

$$\frac{\partial \psi_l}{\partial r} = -\beta \psi_l \text{ at } r = 1\ ,\ l = 1,2 \quad (83)$$

$$\int_0^1 \psi_l r\, dr = 0,\ \ l = 1,2 \quad (84)$$

The equation (80) describes the Strum-Liouville boundary value problem, the solution of which is found using the property of orthogonality of characteristics functions. The characteristic function of the corresponding homogeneous boundary value problem will be orthogonal to the right-hand side of the equation (80) with the weighting function r. So, we find the solution of homogeneous differential equation corresponding to (80) i.e.

$$\frac{1}{r}\frac{\partial}{\partial r}\left(r\frac{\partial \psi_l}{\partial r}\right) + \lambda_0^2 \psi_l = 0 \quad (85)$$

The value of ψ_l from here can be directly calculated using the Bessel's function of zeroth order as $\psi_l = J_0(\lambda_0 r)$.

Let this be denoted by characteristic function $\phi_n = J_0(\lambda_0 r)$ (86)

Now, multiplying both the sides of the equation (80) by $r\phi_n$, the left-hand side of the equation vanishes and using the property of orthogonal of functions, we obtain the value of K_l. The expression for the exchange coefficients $K_l, l = 1,2$ is obtained in terms of the function $\psi_l, l = 1,2$

$$K_l = \frac{\int_0^1 rJ_0(\lambda_0 r)(u\psi_{l-1} - \frac{1}{Pe^2}\psi_{l-2} + \sum_{i=1}^{l} K_i \psi_{l-i})dr}{\int_0^1 \psi_0 r J_0(\lambda_0 r) dr}, \quad l = 1,2 \quad (87)$$

The value of K_1 using (84), (87) in (81)

$$K_1 = \frac{\int_0^1 rJ_0(\lambda_0 r)u\psi_0 dr}{\int_0^1 \psi_0 r J_0(\lambda_0 r) dr} = -\frac{2\lambda_0^2}{(\lambda_0^2+\beta^2)J_0^2(\lambda_0)}\int_0^1 urJ_0^2(\lambda_0 r)dr \quad (88)$$

International Journal of Engineering Technology and Management Sciences
Website: ijetms.in Issue: 2 Volume No.7 March - April – 2023
DOI:10.46647/ijetms.2023.v07i02.052 ISSN: 2581-4621

The value of ψ_1 from (70)

$$\frac{1}{r}\frac{\partial}{\partial r}\left(r\frac{\partial \psi_1}{\partial r}\right) + \lambda_0^2\psi_1 = u\psi_0 + K_1\psi_0 \quad (89)$$

The boundary condition for ψ_1

$$\psi_1 = finite \text{ at } r = 0 \quad (90)$$

$$\frac{\partial \psi_1}{\partial r} = -\beta\psi_1 \text{ at } r = 1 \quad (91)$$

$$\int_0^1 \psi_1 r\, dr = 0 \quad (92)$$

Using the value of K_l in (87), we get the solution of ψ_1 satisfying (90) to (92) as

$$\psi_1 = \sum_{m=0}^{\infty} B_m J_0(\lambda_m r) \quad (93)$$

where the expansion coefficient B_0 using (92) and (93) is obtained in terms of B_j (j=1,2, …..) as

$$B_0 = -\frac{\lambda_0}{J_1(\lambda_0)}\sum_{n=1}^{\infty} B_m \frac{J_1(\lambda_m)}{\lambda_m} \quad (94)$$

Using (94) in (93)

$$\psi_1 = \sum_{m=0}^{\infty} B_m\left(J_0(\lambda_m r) - \frac{\lambda_0}{J_1(\lambda_0)}\frac{J_1(\lambda_m)}{\lambda_m}J_0(\lambda_0 r)\right) \quad (95)$$

Where $B_m = \frac{2\lambda_m^2}{(\lambda_0^2-\lambda_m^2)(\lambda_m^2+\beta^2)J_0^2(\lambda_m)}\int_0^1 (u+K_1)\psi_0 r J_0(\lambda_m r)dr$ (96)

The dispersion coefficient K_2 using (88), (95) and (96) is

$$K_2 = \frac{1}{Pe^2} - \frac{4\lambda_0 J_1(\lambda_0)}{(\lambda_m^2+\beta^2)J_0^2(\lambda_m)}\int_0^1 (u+K_1)\psi_1 r J_0(\lambda_0 r)dr \quad (97)$$

The exchange coefficient K_0 occurring because of the absence of nanoparticle at the capillary wall. The convection coefficient K_1 and dispersion coefficient K_2 are obtained for $\beta \neq 0$, hence they are responsible for the phenomenon of dispersion of nanoparticles in the capillary and the values for which are obtained as

$$K_1 = -2\int_0^1 r\, u\, dr \quad (98)$$

$$K_1 = \frac{2}{3}\left(\frac{hB}{16\mu_f\left(1+2.5\left(1-3.4606\left(\frac{r_p}{R_0}\right)+8.6065\left(\frac{r_p}{R_0}\right)^2\right)\phi\right)}\right)^{\frac{1}{n}}\left(\frac{18n^2+n^4+18n+24n^2+6n^3}{(9-n^2)(3+4n+n^2)}\right) + \frac{16}{hB}\left(\left((1-\phi)+\frac{\phi\rho_p\gamma_p}{\rho_f\gamma_f}\right)Gr\theta + Re\frac{\partial p}{\partial z}\right)\left(\frac{hB}{16\mu_f\left(1+2.5\left(1-3.4606\left(\frac{r_p}{R_0}\right)+8.6065\left(\frac{r_p}{R_0}\right)^2\right)\phi\right)}\right)^{\frac{1}{n}}\left(\frac{9n^2-7n^4-18n^3}{(9-n^2)(9-7n^2-2n^3)}\right) - A \quad (99)$$

Now, $K_2 = \frac{1}{Pe^2} - 2\int_0^1 r\, u\, \psi_1 dr$ (100)

International Journal of Engineering Technology and Management Sciences
Website: ijetms.in Issue: 2 Volume No.7 March - April – 2023
DOI:10.46647/ijetms.2023.v07i02.052 ISSN: 2581-4621

$$K_2 = \frac{1}{Pe^2} - 2\left(\frac{hB}{16\mu_f\left(1+2.5\left(1-3.4606\left(\frac{r_p}{R_0}\right)+8.6065\left(\frac{r_p}{R_0}\right)^2\right)\phi\right)}\right)^{\frac{1}{n}} \sum_{l=1}^{\infty} B_l \left(\frac{n^2}{(3-n)(3+3n)} - \frac{\lambda_l^2 n^2}{4(3-n)(3+5n)} + \frac{\lambda_l^4 n^2}{64(3-n)(3+7n)} - \frac{2n}{(3-n)(3+n)} + \frac{\lambda_l^2 n}{2(3-n)(3+3n)} - \frac{\lambda_l^4 n}{32(3-n)(3+5n)}\right) + \frac{16}{hB}\left(\left((1-\phi) + \frac{\phi\rho_p\gamma_p}{\rho_f\gamma_f}\right) Gr\theta + Re\frac{\partial p}{\partial z}\right)\left(\frac{hB}{16\mu_f\left(1+2.5\left(1-3.4606\left(\frac{r_p}{R_0}\right)+8.6065\left(\frac{r_p}{R_0}\right)^2\right)\phi\right)}\right)^{\frac{1}{n}} \sum_{l=1}^{\infty} B_l \left(\frac{n^2}{(3-n)(3+3n)} - \frac{\lambda_l^2 n^2}{4(3-n)(3+3n)} + \frac{\lambda_l^4 n^2}{64(3-n)(3+5n)} - \frac{2n^3}{(1-n)(3+n)(3+3n)} + \frac{\lambda_l^2 n^3}{2(3+n)(1-n)(3+5n)} - \frac{\lambda_l^4 n^3}{32(3+n)(3+7n)(1-n)}\right) + A\sum_{l=1}^{\infty} B_l \left(1 - \frac{\lambda_l^2}{8} + \frac{\lambda_l^4}{144}\right) + \sum_{l=1}^{\infty} B_l \left(\frac{2\lambda_0 J_1(\lambda_l)}{J_1(\lambda_0)\lambda_l}\left(\frac{hB}{16\mu_f\left(1+2.5\left(1-3.4606\left(\frac{r_p}{R_0}\right)+8.6065\left(\frac{r_p}{R_0}\right)^2\right)\phi\right)}\right)^{\frac{1}{n}} \left(\frac{n^2}{(3-n)(3+3n)} - \frac{\lambda_0^2 n^2}{4(3-n)(3+5n)} + \frac{\lambda_0^4 n^2}{64(3-n)(3+7n)} - \frac{2n}{(3-n)(3+n)} + \frac{\lambda_0^2 n}{2(3-n)(3+3n)} - \frac{\lambda_0^4 n}{32(3-n)(3+5n)}\right)\right) - \frac{16}{hB}\left(\left((1-\phi) + \frac{\phi\rho_p\gamma_p}{\rho_f\gamma_f}\right) Gr\theta + Re\frac{\partial p}{\partial z}\right)\left(\frac{hB}{16\mu_f\left(1+2.5\left(1-3.4606\left(\frac{r_p}{R_0}\right)+8.6065\left(\frac{r_p}{R_0}\right)^2\right)\phi\right)}\right)^{\frac{1}{n}} \sum_{l=1}^{\infty} B_l \left(\frac{\lambda_0 J_1(\lambda_l)}{J_1(\lambda_0)\lambda_l}\left(\frac{B}{16\mu_f\left(1+2.5\left(1-3.4606\left(\frac{r_p}{R_0}\right)+8.6065\left(\frac{r_p}{R_0}\right)^2\right)\phi\right)}\right)^{\frac{1}{n}} \left(\frac{(3-n}{\lambda_0^2 n^2}\right.\right.$$

$$\left.\left.\frac{\lambda_0^2 n^2}{4(3-n)(3+5n)} + \frac{\lambda_0^4 n^2}{64(3-n)(3+7n)} - \frac{2n^3}{(3-n)(3+n)} + \frac{\lambda_0^2 n^3}{2(3-n)(3+3n)} - \frac{\lambda_0^4 n^3}{32(3-n)(3+5n)}\right)\right) - A\sum_{l=1}^{\infty} B_l \left(\frac{\lambda_0 J_1(\lambda_l)}{J_1(\lambda_0)\lambda_l}\left(1 - \frac{\lambda_l^2}{8} + \frac{\lambda_l^4}{144}\right)\right) \quad (101)$$

Where $A = \frac{8}{nh\left((1-\phi)+\frac{\phi\rho_p\gamma_p}{\rho_f\gamma_f}\right)\left((3\phi-1)\frac{k_p}{k_f}+[3(1-\phi)-1]+\sqrt{\{(3\phi-1)\frac{k_p}{k_f}+[(3(1-\phi)-1]\}^2+8\frac{k_p}{k_f}}\right)}\left(\left((1-\phi)+\frac{\phi\rho_p\gamma_p}{\rho_f\gamma_f}\right) Re\frac{\partial p}{\partial z}\right)\left(\frac{h\left((1-\phi)+\frac{\phi\rho_p\gamma_p}{\rho_f\gamma_f}\right)\left((3\phi-1)\frac{k_p}{k_f}+[3(1-\phi)-1]+\sqrt{\{(3\phi-1)\frac{k_p}{k_f}+[(3(1-\phi)-1]\}^2+8\frac{k_p}{k_f}}\right)}{16\mu_f\left(1+2.5\left(1-3.4606\left(\frac{r_p}{R_0}\right)+8.6065\left(\frac{r_p}{R_0}\right)^2\right)\phi\right)}\right)^{\frac{1}{n}}\left(\frac{4n-9n^2+n^3}{(9-n^2)(1-n)}\right) - \left(\frac{h\left((1-\phi)+\frac{\phi\rho_p\gamma_p}{\rho_f\gamma_f}\right)\left((3\phi-1)\frac{k_p}{k_f}+[3(1-\phi)-1]+\sqrt{\{(3\phi-1)\frac{k_p}{k_f}+[(3(1-\phi)-1]\}^2+8\frac{k_p}{k_f}}\right)}{16\mu_f\left(1+2.5\left(1-3.4606\left(\frac{r_p}{R_0}\right)+8.6065\left(\frac{r_p}{R_0}\right)^2\right)\phi\right)}\right)^{\frac{1}{n}}\left(\frac{n-n^2-6}{9-n^2}\right) + u_B$ (102)

International Journal of Engineering Technology and Management Sciences
Website: ijetms.in Issue: 2 Volume No.7 March - April – 2023
DOI:10.46647/ijetms.2023.v07i02.052 ISSN: 2581-4621

$$B = \left((1-\phi) + \frac{\phi\rho_p\gamma_p}{\rho_f\gamma_f}\right) Gr\theta \left((3\phi-1)\frac{k_p}{k_f} + [3(1-\phi)-1] + \sqrt{\{(3\phi-1)\frac{k_p}{k_f} + [(3(1-\phi)-1]\}^2 + 8\frac{k_p}{k_f}}\right) \quad (103)$$

2.3.1.3 Solution for mean concentration

The equation (51) is solved using the boundary conditions (56) and (61) to get

$$c_m = \frac{1}{2Pe\sqrt{\pi T}} \exp(\Lambda - \frac{z_1^2}{4T}) \quad (104)$$

Where $\Lambda(t) = \int_0^t K_0(\eta)d\eta$ (105)

$$z_1(t,z) = z + \int_0^t K_1(\eta)d\eta \quad (106)$$

$$T(t) = \int_0^t K_2(\eta)d\eta \quad (107)$$

We have considered large time interval to analyse the dispersion model. So, the approximation of equations (95) to (97) for large time can be represented as

$$\Lambda(t) \sim K_0 t \quad (108)$$

$$z_1(t,z) \sim z + K_1 t \quad (109)$$

$$T(t) \sim K_2 t \quad (110)$$

2.4 Convergence of solution

Convergence plays an important role in determining the accuracy of the solution. In this problem we have calculated the value of $\psi_i(t,r), i = 0,1,2,\ldots$ which is a function of time and radial distance. The value of ψ_1 is in the form of Bessel function. The convergence of the Bessel function exits in the form of power series solution, but, it does not guarantee the existence of solution to inhomogeneous Bessel differential equation [36] as in equation number (80). Using equation number (93)

$\psi_1 = \sum_{m=0}^{\infty} B_m J_0(\lambda_m r)$

Lemma 1:- If ψ_1/r has bounded variation in the interval $0 \le r \le 1$ then $\int_0^1 \psi_1 J_0(\lambda_m r) = \kappa \frac{\varphi(\lambda_m)}{\lambda_m^{3/2}}$

Proof:- Using the basic properties of Bessel functions, we have

$$J_0(r) = (\frac{2}{\pi r})^{1/2} \left\{\cos\left(r - \frac{\pi}{4}\right) + \kappa\frac{\varphi(0,r)}{r}\right\} \quad (111)$$

Let $\varphi = \frac{\psi_1}{r}$, then

$$\int_0^1 \psi_1 J_0(\lambda_m r)dr = (\frac{2}{\pi\lambda_m})^{1/2} \int_0^1 \vartheta(r) r^{\frac{1}{2}} \cos(\lambda_m r - \frac{\pi}{4})dr + \kappa\frac{\varphi}{\lambda_m^{3/2}} \quad (112)$$

ϑ will be monotonically increasing if $\vartheta = \vartheta_1(r) - \vartheta_2(r)$ in which $\vartheta_1(r)$ and $\vartheta_2(r)$ are also monotonically increasing. Hence,

$$\int_0^1 \vartheta(r) r^{\frac{1}{2}} \cos(\lambda_m r - \frac{\pi}{4})dr = \vartheta(1+0)\int_0^{\varepsilon} r^{\frac{1}{2}} \cos\left(\lambda_m r - \frac{\pi}{4}\right)dr + \vartheta(1-0)\int_{\varepsilon}^1 r^{\frac{1}{2}} \cos\left(\lambda_m r - \frac{\pi}{4}\right)dr = \kappa\frac{\varphi(\lambda_m)}{\lambda_m} \quad (113)$$

Lemma 2:- In the interval $0 \le r \le 1$, let the function ψ_1 be absolutely continuous and let ψ_1' has bounded variation. Then, the general coefficient B_m of the series in (93) may be written as:-

$\frac{(2\pi)^{1/2}\delta_i\psi_1(1)(-1)^m}{\lambda_m^{1/2}} + \kappa\frac{\varphi(\lambda_m)}{\lambda_m^{3/2}}$ where $\delta_i = \begin{cases} 0 \; when \; i \neq 0 \\ 1 \; when \; i = 0 \end{cases}$

Proof:- Using the property of Bessel function we have

$$\int_0^1 r J_0^2(\lambda_m r)dr = \frac{1}{2}[J_0^2(\lambda_m) + J_1^2(\lambda_m)] \quad (114)$$

International Journal of Engineering Technology and Management Sciences
Website: ijetms.in Issue: 2 Volume No.7 March - April – 2023
DOI:10.46647/ijetms.2023.v07i02.052 ISSN: 2581-4621

Using (111)

$$\int_0^1 rJ_0^2(\lambda_m r)dr = \frac{1}{\pi\lambda_m} + \kappa\frac{\varphi_1(\lambda_m)}{\lambda_m^2} \quad (115)$$

By (115), B_m in (93) assumes the form

$$[\lambda_m\pi + \kappa\varphi_1(\lambda_m)]\int_0^1 r\psi_1 J_0(\lambda_m r)dr \quad (116)$$

On integrating using the recurrence formula

$$\frac{d}{dr}[rJ_1(r)] = rJ_0(r) \quad (117)$$

The integral (116) becomes

$$\int_0^1 r\psi_1 J_0(\lambda_m r)dr = \frac{1}{\lambda_m}\int_0^1 \frac{r\psi_1}{(\lambda_m r)} d[(\lambda_m r)J_1(\lambda_m r)] \quad (118)$$

$$= \frac{\psi_1(1)J_1(\lambda_m)}{\lambda_m} - \frac{1}{\lambda_m}\int_0^1 r\psi'_1 J_1(\lambda_m r)dr \quad (119)$$

If we assume $\psi'_1 \geq 0$ and monotonically increasing, thus, $\frac{1}{r}[\psi_1(r) - \psi_1(0)] \geq 0$ is monotonically increasing. It follows that in (119) the integral $\frac{1}{\lambda_m}\int_0^1 r\psi'_1 J_1(\lambda_m r)dr$ has the form $\kappa\frac{\varphi(\lambda_m)}{\lambda_m^{5/2}}$.

Now the term $\frac{\psi_1(1)J_1(\lambda_m)}{\lambda_m}$

$$\lambda_m = m\pi + q + \kappa\frac{\varphi}{m} = \kappa\gamma(m).m \quad 1 \leq \gamma(m) \leq 2 \quad (120)$$

$$\text{Where } q = \begin{cases} \chi\pi - \frac{\pi}{2} + \frac{\pi}{4} & i = 0 \\ \chi\pi + \frac{\pi}{4} & i \neq 0 \end{cases} \quad \chi \text{ is an integer} \quad (121)$$

From (120)

$$\sin(\lambda_m - \tfrac{\pi}{4}) = \sin\left(m\pi + q - \tfrac{\pi}{4}\right) + \kappa\frac{\varphi(m)}{m} \quad (122)$$

$$= \begin{cases} \pm(-1)^m + \chi\frac{\varphi(m)}{m} & i = 0 \\ \kappa\frac{\varphi(m)}{m} & i \neq 0 \end{cases} \quad (123)$$

And (111) gives

$$J_1(\lambda_m) = \delta_i(-1)^m\left(\frac{2}{\pi\lambda_m}\right)^{1/2} + \kappa\frac{\varphi}{\lambda_m^{3/2}} \quad (124)$$

Theorem:- Let ψ_1 be a function as described in *lemma 2* and in addition let the condition $\delta_i\psi_1(1) = 0$ be satisfied then $\psi_1 - S_m(r) = \kappa\frac{\varphi(m,r)}{m^{1/2}}$ in $0 \leq r \leq 1$ where $S_m(r)$ is the sum of first m regular terms of the series ψ_1.

Proof:- It has been shown in *Lemma 1* that the series will converge to the value of the function in any subinterval of $0 \leq r \leq 1$. If $\psi_1(r)$ is continuous in this subinterval and $\delta_i\psi_1(1) = 0$, therefore under the conditions of the theorem the series will converge to ψ_1 in $0 \leq r \leq 1$. Further, from *lemma 2*, the general terms of the series can be expressed as $\kappa\frac{\varphi(\lambda_m)}{\lambda_m^{\frac{3}{2}}}J_0(\lambda_m r)$ where $J_0(\lambda_m r)$ is uniformly bounded and the remainder after m terms is written as $\kappa\frac{\varphi(m)}{m^{1/2}}$. Thus, ψ_1 is convergent in $0 \leq r \leq 1$.

In the above method we described a condition on the remainder after m terms, which is a stronger condition for the convergence of the inhomogeneous solution of the Bessel function. Thus, the solution $\psi_1 = \sum_{m=0}^{\infty} B_m J_0(\lambda_m r)$ obtained for the equation converges.

3. Results and discussions

The present mathematical investigation analyses the dispersion of nanoparticles in capillaries using power law model, over steady state conditions. The temperature of the nanofluid has been analysed for different values of heat source parameter and volume fraction of nanoparticles. The effects of heat

DOI:10.46647/ijetms.2023.v07i02.052 ISSN: 2581-4621

source parameter, volume fraction of nanoparticles, power law index, radius of nanoparticle, Grashof number, Darcy number and slip parameter has been observed on velocity of nanofluid.

We have employed the method adopted by Sankarsubramanian and Gill [6] and obtained the effects of parameters like heat source parameter, power law index, radius of nanoparticle and Grashof number on the exchange coefficient, convection coefficient and dispersion coefficient during nanoparticle dispersion under steady state conditions with small values of wall absorption parameter. The small values of wall absorption parameter signify small or no reaction rates at the healthy vessel wall. This would justify the fact that as the nanoparticles move towards the wall their concentration at the wall will not become zero for healthy cells at the wall and hence, they can disperse into the diseased cells which will have a higher value of absorption parameter than the healthy cells. Thus, the nanoparticle can be used for diseased cell targeting.

Fig 2 displays the effects of temperature θ of nanofluid against radial direction r for different values of heat source parameter h . The temperature drops with the increase in radial co-ordinates. This is because nanoparticles convect radially from higher temperature gradient to lower temperature gradient. It is seen from Fig 2 that higher the value of heat source parameter h, greater the temperature of the nanofluid. This is because the increase in the value of heat source parameter signifies greater heat production in the nanofluid [37] due to nanoparticle Brownian motion. Thus, the temperature of nanofluid rises with the increase in heat source parameter.

Fig 3 depicts the effects of temperature θ of nanofluid against radial direction r for different values of volume fraction ϕ of nanoparticles. The trend shows that higher the value of volume fraction, greater the temperature of the nanofluid. The volume fraction of nanoparticles represents the number of nanoparticles in the nanofluid. Thus, higher the value of volume fraction, greater the temperature owing to increase in the number of nanoparticles, hence the rise in temperature. Similar results were reported by Tan et al [38].

Fig 4 shows the graph of velocity u of nanofluid against radial direction r for different values of heat source parameter h . The rise in the value of heat source parameter, raises the temperature of the nanofluid which in turn causes a rise in the velocity of the nanofluid due to higher heat generation [37]. Thus, the velocity rises with the increase in heat source parameter.

Fig 5 shows the graph of velocity u of nanofluid against radial direction r for different values of volume fraction ϕ of nanoparticles. The trend shows decrease in velocity with increase in the volume fraction.

Higher value of volume fraction signifies higher number of nanoparticles in the nanofluid. The greater number of nanoparticles experience greater collision amongst themselves, thus decreasing the value of velocity of nanofluid [37].

Fig 6 shows the graph of velocity u of nanofluid against radial direction r for different values of power law index n. The trend depicts that higher value of power law index causes a decrease in the velocity of nanofluid. Power law index represents shear thinning fluids for values lesser than unity. This behaviour is observed because of the nanoparticles dispersed in the blood. Nanoparticles tend to form loose aggregates which is broken rapidly by increasing shear rates. This causes a reduction in their resistance to flow. Thus, the velocity of nanofluid decreases with the increase in the power law index [24].

Fig 7 displays the graph of velocity u of nanofluid against radial direction r for different values of nanoparticle radius r_p. The nature of the graph shows that decrease in the value of nanoparticle radius increases the velocity of the nanofluid. The viscosity dependence relation given by Pasol and Feuillebois [29] directly relates the viscosity with the radius of nanoparticle. And viscosity is inversely related to velocity for shear thinning fluids as the case considered here. Nanoparticle radius governs the size of nanoparticle. Higher the radius, greater the size of the nanoparticle. The greater size of nanoparticle causes a reduction in velocity, thus the result.

Fig 8 exhibits the graph of velocity u of nanofluid against radial direction r for different values of Grashof number Gr. The trend shows that the velocity increases with the increase in the value of

DOI:10.46647/ijetms.2023.v07i02.052 ISSN: 2581-4621

Grashof number. Grashof number is the ratio of buoyant forces to viscous forces. Buoyant forces are caused in the nanofluid due to the temperature gradient, as there will be no flow in the absence of it. Thus, higher the value of Grashof number, higher the temperature, that in turn causes a higher velocity [37].

Fig 9 displays the graph of velocity u of nanofluid against radial direction r for different values of Darcy number Da. The graph shows that the velocity increases with the increase in the value of Darcy number. Darcy number represents the permeability of the medium across the cross-sectional area of fluid flow. As the value of Dracy number increases, the fluid flow becomes stronger due to increase in the permeability of the medium [37]. Thus, increase in Darcy number causes an increase in the velocity of the nanofluid.

Fig 10 shows the graph of velocity u of nanofluid against radial direction r for different values of slip parameter σ. It is seen that an increase in the value of slip parameter causes a decrease in the velocity of the nanofluid. Slip parameter represents the fluid slip at the boundary of the capillary wall. The increase in its value causes a decrease in the skin friction and heat transfer, thus deceasing the velocity of the nanofluid [39].

Fig 11 exhibits the graph of exchange coefficient $-K_0$ against wall absorption parameter β. The graphs shows that exchange coefficient K_0 increases with the increase in wall absorption parameter β. K_0 signifies the reaction rate constant depending on time. As it is a steady state, K_0 depends only on ψ_0. ψ_0 describes the dispersion of nanoparticles in the capillary for first order homogeneous reactions. Wall absorption parameter β represents the nanoparticle concentration that builds up at the wall of the capillary as they are dispersed. Thus, the reaction rate constant depends directly on the rate at which nanoparticles are absorbed at the capillary wall [6] [40]. Hence K_0 increases with the increase in β.

Fig 12 exhibits the graph of convection coefficient $-K_1$ against wall absorption parameter β for different values of heat source parameter h. Convection coefficient enhances with the increase in wall absorption parameter because nanoparticles begin convections rapidly towards the capillary wall due to there increased interactions at the wall of capillary [40]. The graph shows that an increase in the value of heat source parameter h causes an increase in $-K_1$. Since heat source parameter relies on the heat production due to nanoparticle collisions, an increase in its value increases the dispersion of nanoparticles in the fluid. Thus, the value of convection coefficient increases with the increase in the value of heat source parameter.

Fig 13 shows the graph of convection coefficient $-K_1$ against wall absorption parameter β for different values of power law index n. It is seen that an increase in the value of power law index causes a decrease in convection coefficient. Power law index describes the rheology of the nanofluid. Nanoparticles behave like suspensions, thus nanofluid shows shear thinning properties under low shear rates. Since it is a shear thinning fluid, as the value of power law index decreases, nanoparticles gradually align themselves in the direction of increasing shear and thus impedance to flow is reduced. As a result, nanoparticles start convections faster towards the capillary wall [40]. Thus, the convection coefficient $-K_1$ increases as the value of power law index n decreases.

Fig 14 displays the trend of convection coefficient $-K_1$ against wall absorption parameter β for different values of nanoparticle radius r_p. From the graph it is seen that an increase in the value of nanoparticle radius causes a decline in the convection coefficient. The radius of nanoparticle chiefly defines the size of nanoparticle dispersed in the nanofluid. Greater the size, more will be impedance to flow, thus slower will be the convection. Hence the result. This implies that that the physical properties of nanoparticles hold considerable importance in their dispersion [41].

Fig 15 shows the graph of convection coefficient $-K_1$ against wall absorption parameter β for different values of Grashof number Gr. It is seen that an increase in the value of Grashof number causes an increase in convection coefficient. Grashof number arises due to convection. Thus, higher the value of Grashof number, greater the convections.

International Journal of Engineering Technology and Management Sciences
Website: ijetms.in Issue: 2 Volume No.7 March - April – 2023
DOI:10.46647/ijetms.2023.v07i02.052 ISSN: 2581-4621

Fig 16 exhibits the graph of dispersion coefficient $-K_2$ against wall absorption parameter β for different values of heat source parameter h. Dispersion coefficient decreases with the increase in wall absorption parameter. The velocity gradient is smaller in the central region of the capillary than near the capillary wall [6]. The nanoparticles tend to disperse more towards the capillary wall with the increasing wall absorption parameter, increasing the transverse movements towards the wall, and thus decreasing the axial dispersion coefficient [6]. The graph also shows that an increase in the value of heat source parameter causes an increase in dispersion coefficient. This is because as the value of heat source parameter increases the dispersion is enhanced in the capillary.

Fig 17 exhibits the graph of dispersion coefficient $-K_2$ against wall absorption parameter β for different values of power law index n. It is seen that as the power law index increases, dispersion decreases. Power law index defines shear thinning behaviour for values less than unity. Nanoparticles suspended in nanofluids define the properties of a shear thinning fluid. Therefore, as the value of power law index decreases, the nanofluid becomes less viscous and hence the dispersion increases.

Fig 18 displays the trend of dispersion coefficient $-K_2$ against wall absorption parameter β for different values of nanoparticle radius r_p. From the graph it is seen that an increase in the value of nanoparticle radius causes a decline in the dispersion coefficient. The nanoparticle size gives the measure of nanoparticle coverage which quantifies and qualifies the dispersion. Higher dispersion occurs with smaller nanoparticles because they cause lesser impedance [42]. Thus, greater the size, lesser the dispersion of nanoparticles.

Fig 19 shows the graph of dispersion coefficient $-K_2$ against wall absorption parameter β for different values of Grashof number Gr. It is seen that an increase in the value of Grashof number causes an increase in dispersion coefficient. This is because an increase in Grashof number causes a greater movement of nanoparticles towards the capillary wall [43]. The buoyancy forces enhance dispersion, thus the result.

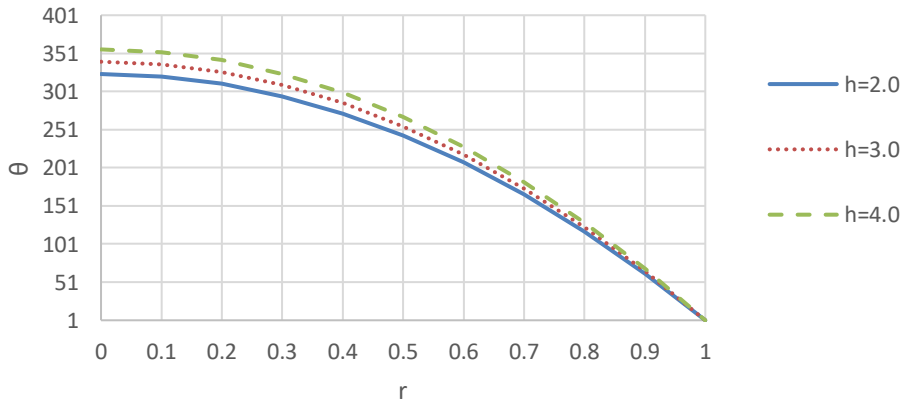

Fig. 2. Variation of temperature θ against radius r for different values of heat source parameter h

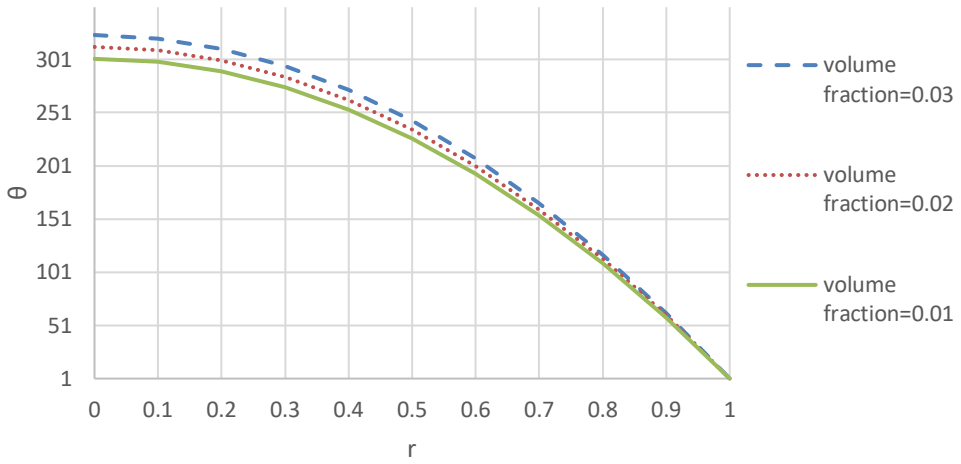

Fig. 3. Variation of temperature θ against radius r for different values of volume fraction φ

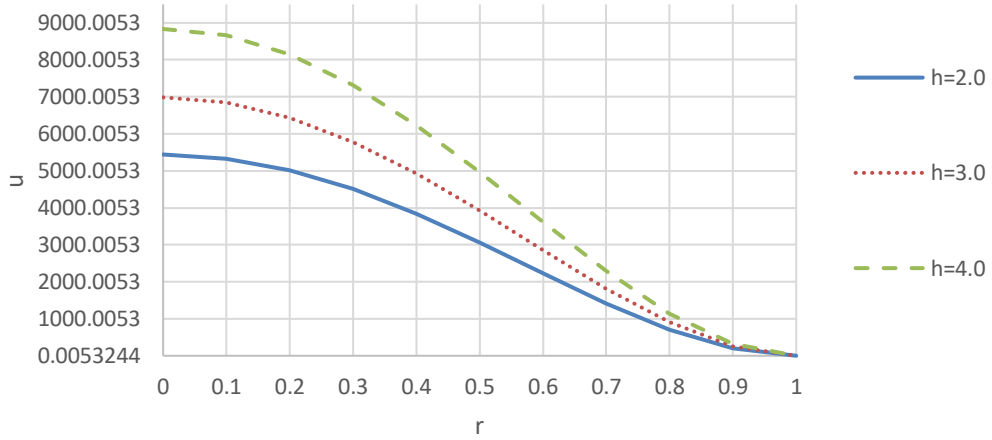

Fig. 4. Variation of velocity u against radius r for different values of heat soure parameter h

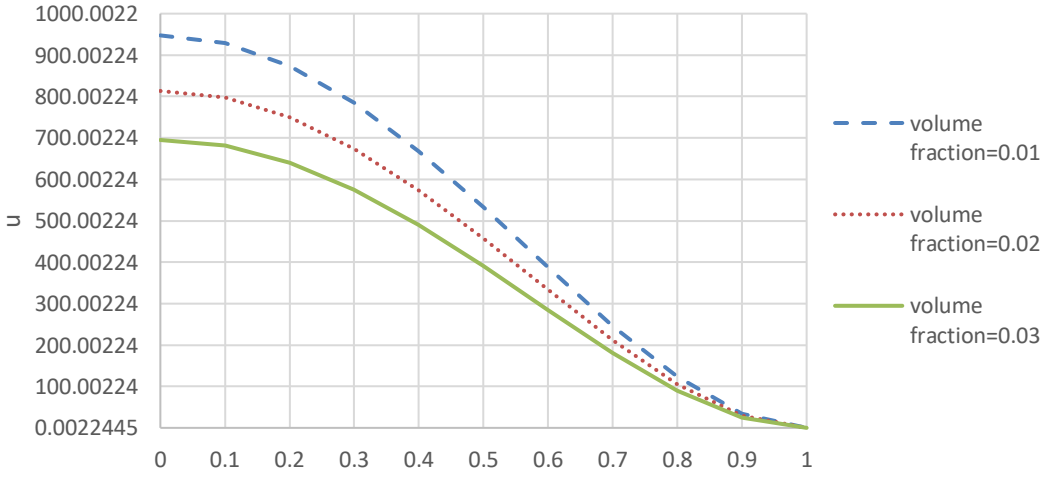

Fig. 5. Variation of velocity u against radius r for different values of volume fraction φ

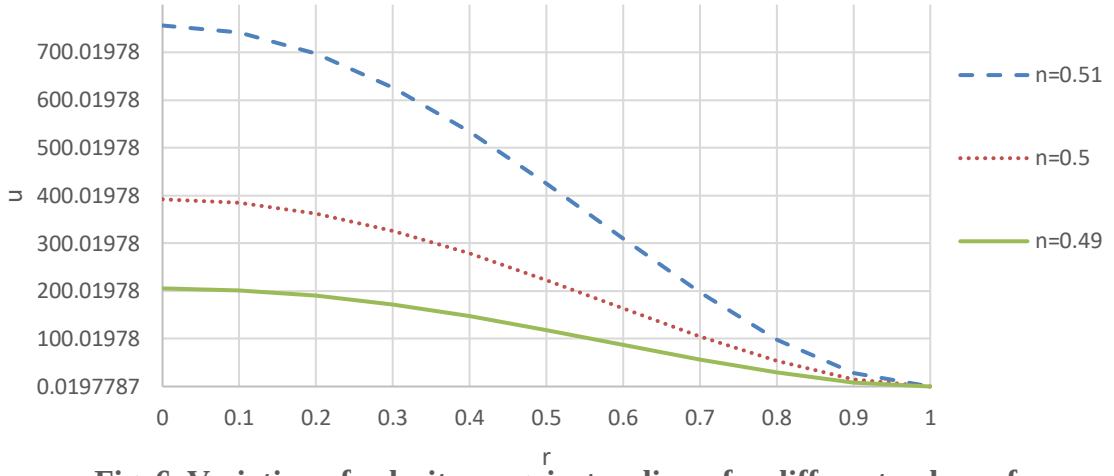

Fig. 6. Variation of velocity u against radius r for different values of powerlaw index n

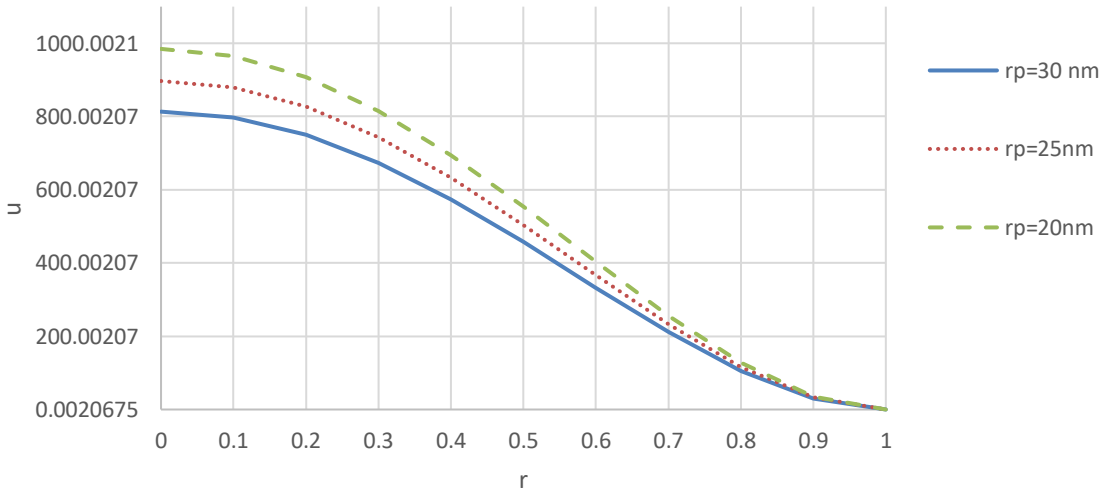

Fig .7. Variation of velocity u against radius r for different values of nanoparticle radius rp

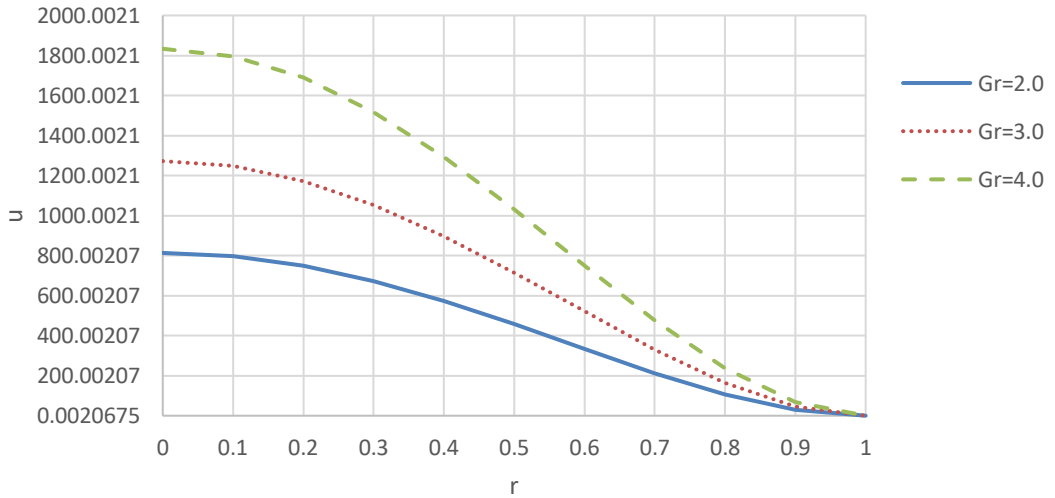

Fig. 8. Variation of velocity u against radius r for different values of Grashof number Gr

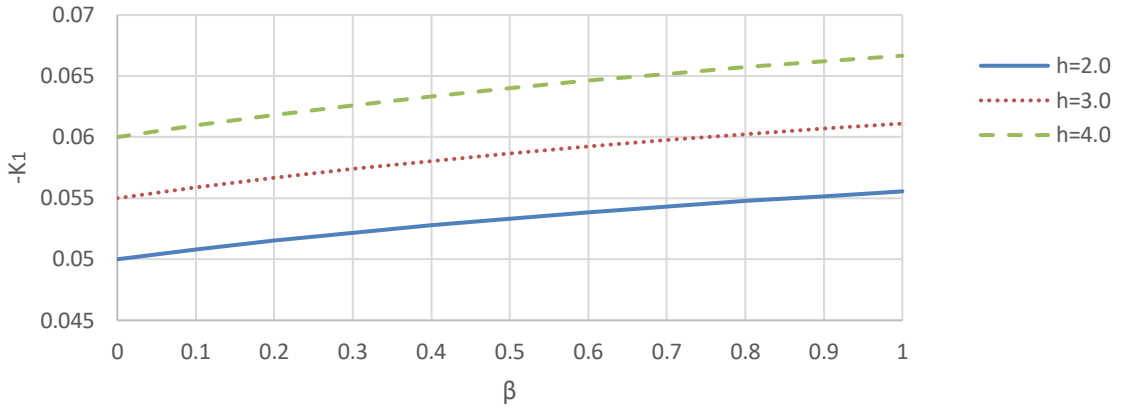

Fig. 12. Variation of convection coefficient -K1 against wall absorption parameter β for different values of heat source parameter h

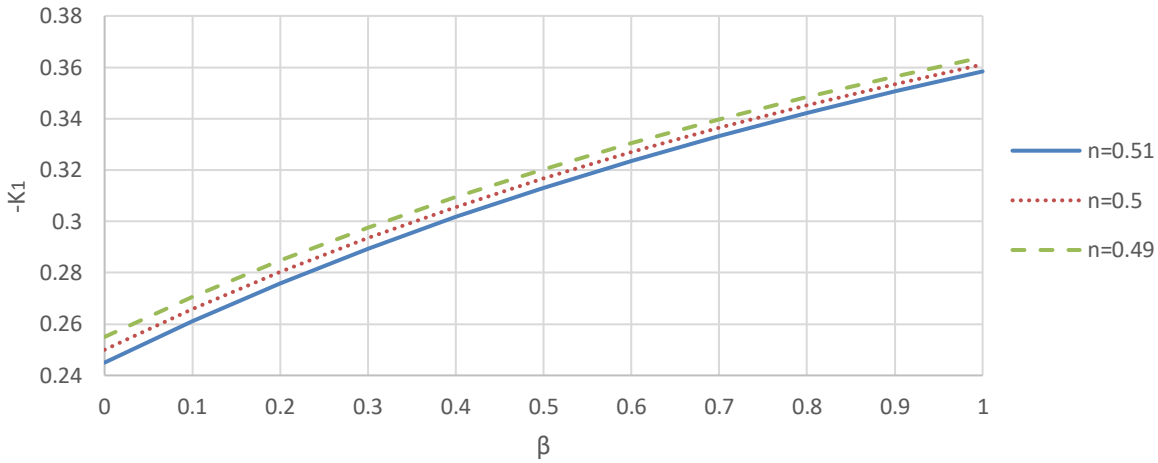

Fig .13. Variation of convection coefficient -K1 against wall absorption parameter β for different values of power law index n

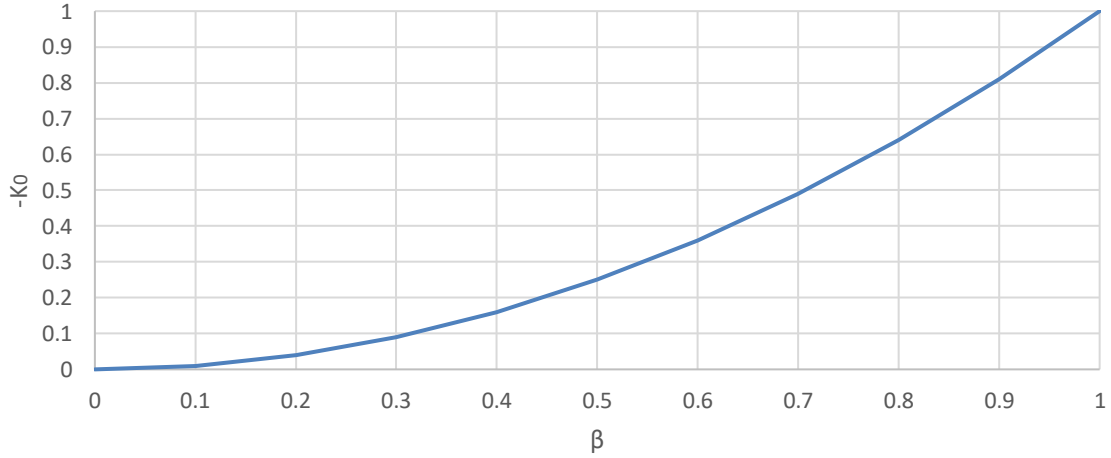

Fig .11. Variation of exchange coefficient -K0 against small values of wall absorption parameter β under steady state condition

International Journal of Engineering Technology and Management Sciences
Website: ijetms.in Issue: 2 Volume No.7 March - April – 2023
DOI:10.46647/ijetms.2023.v07i02.052 ISSN: 2581-4621

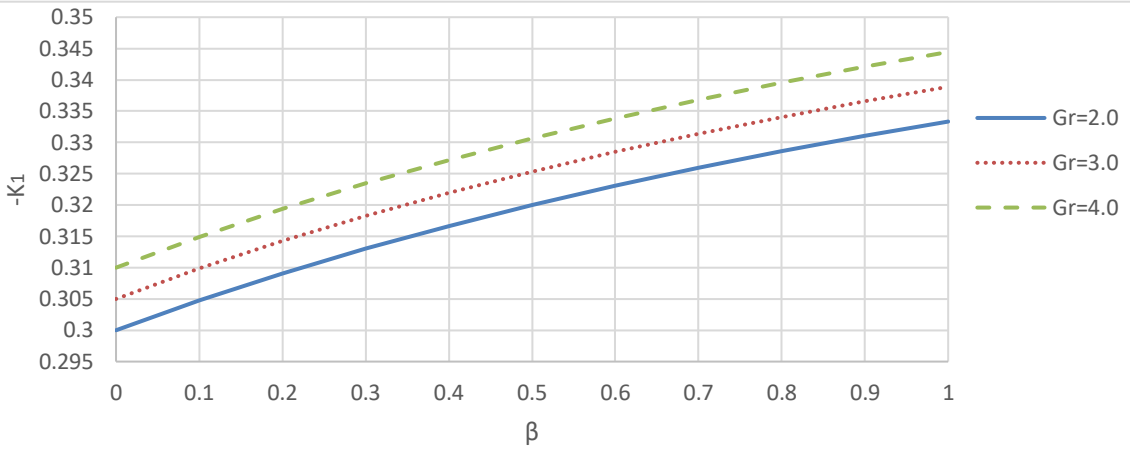

Fig 15 Variation of convection coefficient -K1 against wall absorption parameter β for different values of Grashof number Gr

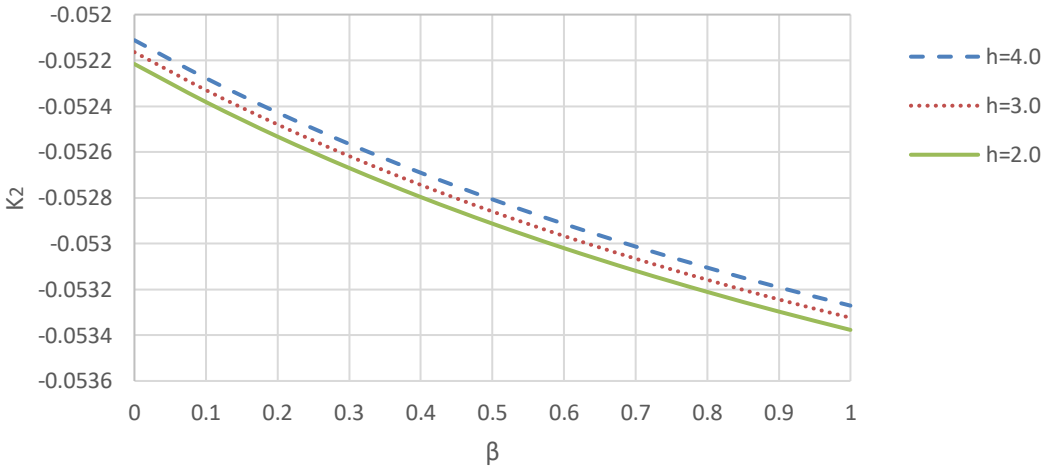

Fig. 16. Variation of dispersion coefficient -K2 against wall absorption parameter β for different values of heat source parameter h

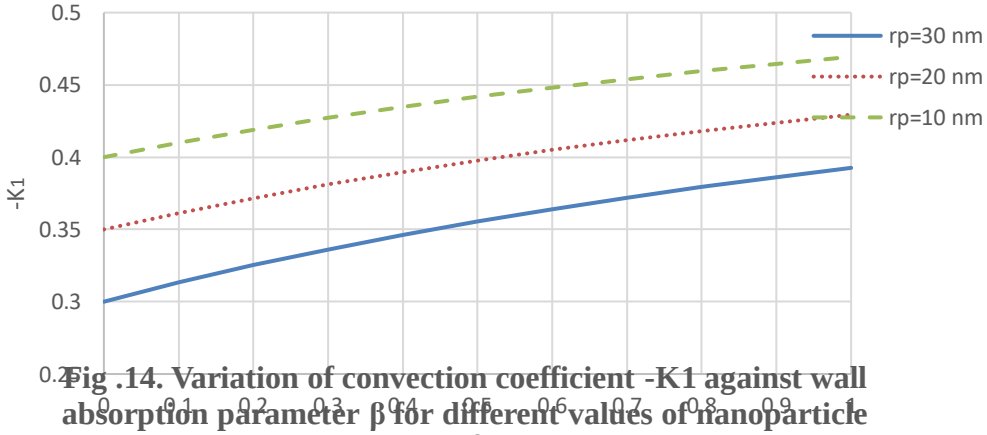

Fig .14. Variation of convection coefficient -K1 against wall absorption parameter β for different values of nanoparticle radius rp

International Journal of Engineering Technology and Management Sciences
Website: ijetms.in Issue: 2 Volume No.7 March - April – 2023
DOI:10.46647/ijetms.2023.v07i02.052 ISSN: 2581-4621

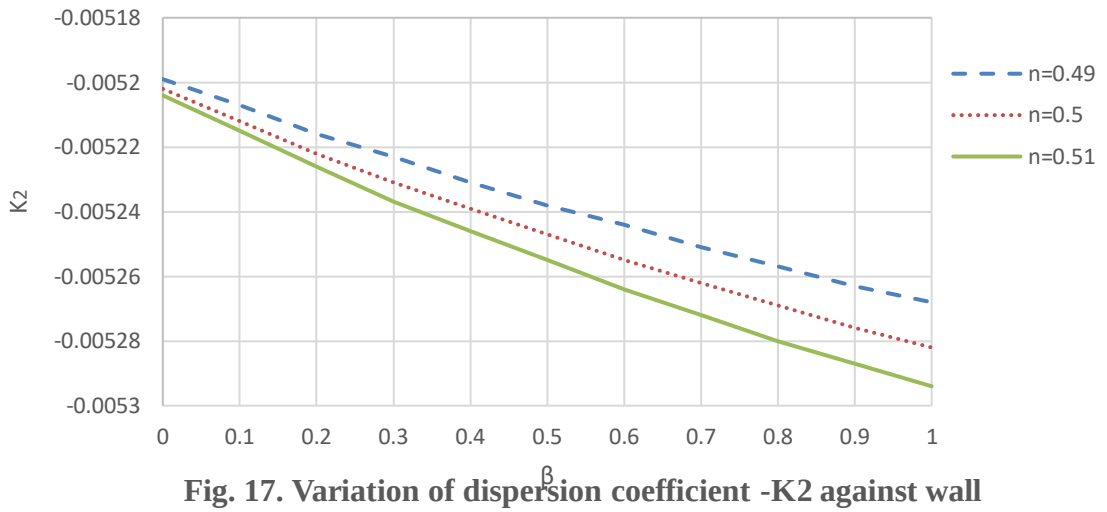

Fig. 17. Variation of dispersion coefficient -K2 against wall absorption parameter β for different values of power law index n

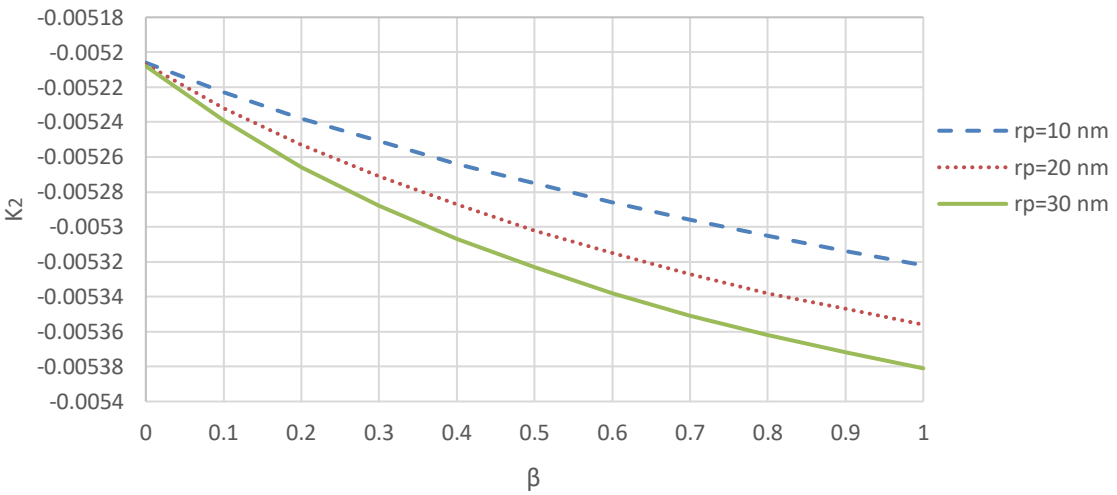

Fig. 18. Variation of dispersion coefficient -K2 against wall absorption parameter β for different values of nanoparticle radius rp

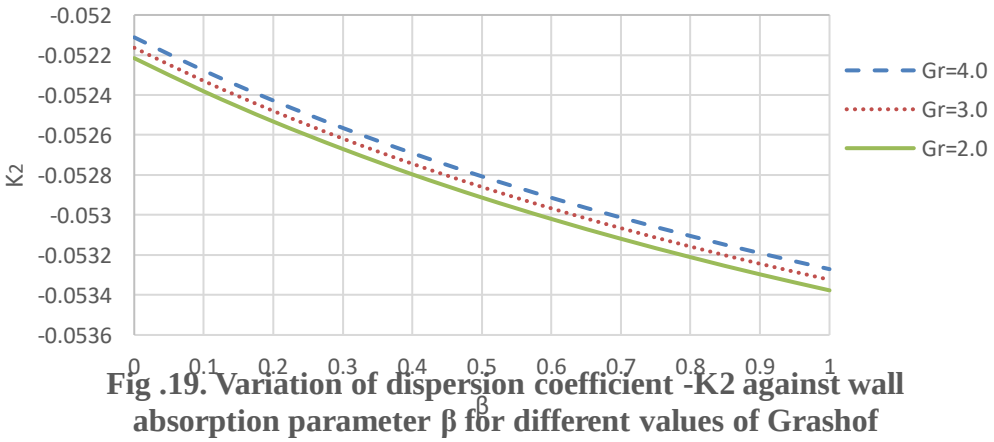

Fig .19. Variation of dispersion coefficient -K2 against wall absorption parameter β for different values of Grashof number Gr

DOI:10.46647/ijetms.2023.v07i02.052 ISSN: 2581-4621

4. Conclusion

Nanoparticles have become an exceedingly powerful tool for drug delivery in the treatment pf cardiovascular diseases. The evaluation of standard processes in the field is a major field of research. This paper concerns with the nanoparticle dispersion in capillaries using power law model. The effect of heat source parameter, volume fraction, power law index, size of nanoparticles, Grashof number, Darcy number and slip parameter for small values of wall absorption parameter under steady state conditions have been examined on temperature, velocity, exchange coefficient, convection coefficient and dispersion coefficient of nanoparticles dispersed in blood capillary. The formula predictions agree well with the experimental designs [44]. The above nanoparticle aspects are important criteria for nanoparticle dispersion in physiological situations. The major findings of the study can be outlined as:-

- The temperature of nanofluid rises with rise in heat source parameter and volume fraction of nanoparticles.
- The velocity of nanofluid enhances with enhance in heat source parameter, Grashof number and Darcy number.
- The velocity of nanofluid declines with an increase in volume fraction, power law index, nanoparticle radius and slip parameter.
- The exchange coefficient boosts with the increase in wall absorption parameter.
- The convection coefficient also grows with rise in wall absorption parameter.
- The convection coefficient elevates with elevation in heat source parameter and Grashof number.
- The convection coefficient decreases with increase in power law index and nanoparticle radius.
- The dispersion coefficient reduces with the increase in wall absorption parameter.
- The dispersion coefficient improves with elevation in heat source parameter and Grashof number.
- The dispersion coefficient subsides with increase in power law index and nanoparticle radius.

This model provides an efficient insight into the physical properties of nanoparticles, most significantly their size, which is important for their dispersion in blood. It has useful application in the treatment of targeted delivery of drugs where nanoparticles can themselves serve as drugs or a suitable drug can be attached to it. In future, the dispersion model discussed here can be extended to study nanoparticle clustering and also their distribution in full vasculature.

References

[1]G Taylor. “Dispersion Of Soluble Matter In Solvent Flowing Slowly Through A Tube”. Proceedings of The Royal Society London A 219, pp 186-203, 1953 DOI:10.1098/rspa.1953.0139
[2]R Aris. “On The Dispersion Of A Solute In A Fluid Flowing Through A Tube”. Proceedings of The Royal Society London A 235, pp 67-77, 1956 DOI:10.1098/rspa.1956.0065
[3]W N Gill and R Sankarsubramanian. “Exact Analysis Of Unsteady Convective Diffusion.” Proceedings of The Royal Society London A 316, pp 341-350, 1970 DOI:10.1098/rspa.1971.0083
[4]R Sankarsubramanian and W N Gill. “Dispersion Of Non-Uniform Slug In Time-Dependent Flow” Proceedings of The Royal Society London A 322, pp 101-117, 1971 DOI:10.1098/rspa.1971.0057
[5]R Sankarsubramanian and W N Gill. “Dispersion From A Prescribed Concentration In Time Variable Flow.” Proceedings of The Royal Society London 329, pp 479-492, 1972 DOI:10.1098/rspa.1972.0125
[6]R Sankarsubramanian and W N Gill. “Unsteady Convective Diffusion With Interphase Mass Transfer.” Proceedings of The Royal Society London A 833, pp 115-132, 1973 DOI:10.1098/rspa.1973.0051
[7]R Sankarsubramanian and W N Gill. “Corrections to ‘Unsteady convective diffusion with interphase mass transfer’ ”. Proceedings of The Royal Society London A 341, pp 407-408, 1974 DOI:10.1098/rspa.1974.0195

[8]P Decuzzi, F Causa, M Ferrari and A P Netti. "The Effective Dispersion Of Nanovectors Within The Tumour Microvasculature." Annals of Biomedical Engineering 32, pp 798-802, 2006
[9]F Gentile, M Ferrari and P Decuzzi. "The Transport Of Nanoparticles In Blood Vessels: The Effect Of Vessel Permeability And Blood Rheology." Annals of Biomedical Engineering 36, pp 254-261, 2008
[10] F Gentile and P Decuzzi. "Time Dependent Dispersion Of Nanoparticles In Blood Vessels." Journal of Biomedical Science and Engineering 3, pp 517-524, 2010 DOI:10.4236/jbise.2010.35072
[11] S Shaw, S Ganguly, P Sibanda and S Chakraborty. "Dispersion Characteristics Of Blood During Nanoparticle Assisted Drug Delivery Process Through A Permeable Micro Vessel." Microvascular Research 92 pp 25-33, 2014 DOI:10.1016/j.mvr.2013.12.007
[12] R Bali, N Gupta and S Mishra. "Dispersion Characteristics Of Non-Newtonian Fluid During Transportation Of Nanoparticles In Permeable Capillary." Applications and Applied Mathematics Vol 11, Issue 2, pp 632-645, 2016
[13] J V R Reddy, D Srikanth and S K Das. "Modelling And Simulation Of Temperature And Concentration Dispersion In A Couple Stress Nanofluid Flow Through Stenotic Tapered Artery." The European Physical Journal Plus 132:365 , 2017 DOI: 10.1140/epjp/i2017-11643-1
[14] R Bali and N Gupta. "Study Of Transport Of Nanoparticles With K-L Model Through A Stenosed Micro Vessels." Applications and Applied Mathematics Vol 13, Issue 2, pp 1157-1170, 2018
[15] K M Surabhi, J V R Reddy and D Srikanth. "Impact Of Temperature And Concentration Dispersion On The Physiology Of Blood Nanofluid: Links To Atherosclerosis." Indian Academy of Sciences, Sadhana 43:210, 2018 DOI:10.1007/812406-018-0986-8
[16] J V R Reddy and D Srikanth. "Impact Of Blood Vessel Wall Flexibility On The Temperature And Concentration Dispersion." Journal of Applied and Computational Mechanics. Vol 6, Issue 3, pp 564-581, 2020 DOI:10.22055/JACM.2019.29023.1542
[17] S Rathore and D Srikanth. "Mathematical Study Of Transport Phenomena Of Blood Nanofluid In A Diseased Artery Subject To Catheterization." Indian Journal of Physics, 2021 DOI:10.1007/s12648-021-02166-2
[18] S U S Choi and J A Eastman. "Enhancing Thermal Conductivity Of Fluids With Nanoparticle In Developments And Applications Of Non-Newtonian Flows." International mechanical engineering congress and exhibition, San Francisco , U S, Conference, 1995
[19] J Buongiorno. "Convective Transport In Nanofluids." Journal of Heat Transfer, Vol 128, Issue 3, pp 240-250, 2006 DOI:10.1115/1.21150834
[20] A Einstein. "Eine neue bestimmumng der molekuldimensionen." Ann Phys 19,pp 289-306, 1906 DOI:10.1002/andp.19063240204
[21] A Santra, S Sen and N Chakraborty. "Study Of Heat Transfer Due To Laminar Flow Of Copper Water Nanofluid Through Two Isothermally Heated Parallel Plates." International Journal of Thermal Sciences 48, pp 391-400, 2009
[22] T Hayat, M Hussain, S A Shehzad and A Alsaedi. "Flow Of A Power Law Nanofluid Past A Vertical Stretching Sheet With A Convective Boundary Condition" Journal of Applied Mechanical and Technical Physics 57, pp 173-179, 2016
[23] M Khan and W A Khan. "MHD Boundary Layer Flow Of A Power Law Nanofluid With New Flux Condition." AIP Advances 6, pp 2119-2126, 2016
[24] S Hussain, A Aziz, C M Khalique and T Aziz. "Numerical Investigation Of Magnetohydrodynamic Slip Flow Of Power-Law Nanofluid With Temperature Dependent Viscosity And Thermal Conductivity Over A Permeable Surface." De Gruyter Open 15, pp 867-876, 2017 DOI:10.1515/phys-2017-0104
[25] Usman, A Ghaffari, I Mustafa, J Muhammad and Y Altaf. "Analysis Of Entropy Generation In A Power Law Nanofluid Flow Over A Stretchable Rotatory Porous Disk." Case studies in thermal engineering, 2021 DOI:10.1016j.csite.2021.101370

[26] El Mehdi Acchal, H Jabraoui, S Zeroual, H Loulijit, A Hasnaoui and S Ouaskit. "Modelling And Simulations Of Nanofluids Using Classical Molecular Dynamics: Particle Size And Temperature Effects On Thermal Conductivity." Advanced powder technology, 2018 DOI:10.1016/j.apt2018.06.023
[27] B Ankamwar. "Size And Shape Effect On Biomedical Applications Of Nanomaterials." Biomedical Engineering- Technical Applications in Medicine pp 94-114, 2012 DOI:10.5772/46121
[28] S Ganguly and S Chakraborty. "Effective Viscosity Of Nanoscale Colloidal Suspensions." Journal of Applied Physics, 2009
[29] L Pasol and F Feuillibois. "Effective Viscosity Of An Inhomogeneous Dilute Suspensions Flowing In A Wall." XXI International Congress of Theoretical and Applied Mechanics, Warsaw Poland,2004
[30] S Shaw. "Effective Shear Augmented Dispersion Of Solutes During Nanoparticle Ssisted Vdrug Delivery In A Micro Vessel." The Japan society of fluid mechanics, Fluid Dynamics Research. ,2020 DOI:10.1088/1873-70051/ab6617
[31] J C Maxwell. "A Treatise On Electricity And Magnetism". Clarendon Press, Oxford, 1873
[32] D A G Bruggeman. "Berichnung verschiedener physikalischer Konstantein von heterogenen substanzen I Dielektrizitatskonstanten und leiffahigkuten der mischkorpher aus isotropen substanzen." Annals of Physics Vol 416, pp 636-664, 1935 DOI:10.1002/anap.193541560705
[33] B C Pak and Y I Cho. "Hydrodynamics And Heat Transfer Study Of Dispersed Fluids With Submicron Metallic Oxide Particles." Exp heat transfer 11, pp 151-170, 1980 DOI:10.1080/08916159808946559
[34] Y Xuan and W Roetzel. "Conceptions For Heat Transfer Correlation Of Nanofluids." International Journal of Heat Transfer 43, pp 3701-3707, 2000 DOI:10.1016/S0017-9310(99)00369-5
[35] J R Philip. "Numerical Solution Of The Diffusion Type With Diffusivity Concentration Dependent." Division of Plant Industry, CSIRO, Deniliquin, NSW, 1956
[36] M G Scherberg. "The Degree Of Convergence Of A Series Of Bessel Functions." University of Minnesota, Minneapolis. Minn, 1932
[37] S Ijaz and S Nadeem. "Examination Of Nanoparticles As A Drug Carrier On Blood Flow Through Catheterized Composite Stenosed Artery With Permeable Walls." Computer methods and programs in biomedicine, 133, pp 83-94, 2016 DOI:10.1016/j.cpmb.2016.05.004
[38] J Tan, W Keller, S Sohrabi, J Yang and Y Liu. "Characterization Of Nanoparticle Dispersion In Red Blood Cell Suspension By The Lattice Boltzmann-Immersed Boundary Method." Nanomaterials, 6, 30, 2016 DOI:10.3390/nano6020030
[39] D Ramaya, R S Raju, A Rao and A J Chamkha. "Effects Of Velocity And Thermal Wall Slip On Magnetohydrodynamics Boundary Layer Viscous Flow And Heat Transfer Of A Nanofluid Over A Non-Linearly-Stretching Sheet: A Numerical Study." Propulsion and power research. Volume 7, Issue 2, pp 182-195, 2018 DOI:10.1016/j.jppr.2018.04.003
[40] B Ramana and G Sarojamma. "Unsteady Convective Diffusion In A Herschel-Bulkley Fluid In A Conduit With Interphase Mass Transfer." International journal of Mathematical modelling and computations. Vol 2, No.3, pp- 159-179, 2012
[41] J W Shreffler, J E Pullan, K M Dailey, S Mallik and A E Brooks. "Overcoming Hurdles In Nanoparticle Clinical Translation: The Influence Of Experimental Design And Surface Modification." International journal of molecular sciences, 20, 6056, 2019 DOI:10.3390/ijms20236056
[42] T Hupfeld, A Sommereyns and S Barickowski. "Analysis Of The Nanoparticle Dispersion And Its Effects On The Crystalline Microstructure In Carbon-Additivated PA12 Feedstock Material For Laser Powder Bed Fusion." Materials, Multidisciplinary Digital Publishing Institute, 13(15):3312, 2020 DOI: 10.3390/ma13153312
[43] A Mukherjee and B S Mazumder. "Buoyancy Effect On Dispersion Of A Solute In A Flow Through A Horizontal Channel." Acta Mechanica 58, pp 137-152, 1986 DOI:10.007/BF01176596

DOI:10.46647/ijetms.2023.v07i02.052 ISSN: 2581-4621

[44] P Bihari, M Vippola, S Schultes, M Praetner, A G Khandoga, C A Reichel, C Coester, T Tuomi, M Rehberg and F Krombach. "Optimized Dispersion Of Nanoparticles For Biological In Vitro And In Vivo Studies." Particle and Fibre Toxicology, 5:14, 2008 DOI:10.1186/1743-8977-5-14

[45] Shwetasaibal Samanta Sahoo; Mousime Xalxo; B G Mukunda. "A Study on Tourist Behaviour Towards Sustainable Tourism in Karnataka". *International Research Journal on Advanced Science Hub*, 2, 5, 2020, 27-33. doi: 10.47392/irjash.2020.28

[46] Muniyandy Elangovan; Mohamed Yousuf; Mohamed Nauman; Mohammed Nayeem. "Design and Development of Delivery Robot for Commercial Purpose". *International Research Journal on Advanced Science Hub*, 4, 07, 2022, 192-197. doi: 10.47392/irjash.2022.047

[47] Manikandan N; Swaminathan G; Dinesh J; Manish Kumar S; Kishore T; Vignesh R. "Significant Attention in Industry and Academia for Wire Arc Additive Manufacturing (WAAM) - A Review". *International Research Journal on Advanced Science Hub*, 4, 07, 2022, 198-204. doi: 10.47392/irjash.2022.048

[48] Shoeb Ahmed Syed; Steve Ales; Rajesh Kumar Behera; Kamalakanta Muduli. "Challenges, Opportunities and Analysis of the Machining Characteristics in hybrid Aluminium Composites (Al6061-SiC-Al2O3) Produced by Stir Casting Method". *International Research Journal on Advanced Science Hub*, 4, 08, 2022, 205-216. doi: 10.47392/irjash.2022.051

[49] Ashima Saxena; Preeti Chawla. "A Study on the Role of Demographic Variables on Online Payment in Delhi NCR". *International Research Journal on Advanced Science Hub*, 4, 08, 2022, 217-221. doi: 10.47392/irjash.2022.052

[50] Vishnupriya S; Nirsandh Ganesan; Ms. Piriyanga; Kiruthiga Devi. "Introducing Fuzzy Logic for Software Reliability Admeasurement". *International Research Journal on Advanced Science Hub*, 4, 09, 2022, 222-226. doi: 10.47392/irjash.2022.056

[51] GANESAN M; Mahesh G; Baskar N. "An user friendly Scheme of Numerical Representation for Music Chords". *International Research Journal on Advanced Science Hub*, 4, 09, 2022, 227-236. doi: 10.47392/irjash.2022.057

[52] Nirsandh Ganesan; Nithya Sri Chandrasekar; Ms. Gokila; Ms. Varsha. "Decision Model Based Reliability Prediction Framework". *International Research Journal on Advanced Science Hub*, 4, 10, 2022, 236-242. doi: 10.47392/irjash.2022.061

[53] Vishnupriya S; Nithya Sri Chandrasekar; Nirsandh Ganesan; Ms. Mithilaa; Ms. Jeyashree. "Comprehensive Analysis of Power and Handloom Market Failures and Potential Regrowth Options". *International Research Journal on Advanced Science Hub*, 4, 10, 2022, 243-250. doi: 10.47392/irjash.2022.062

[54] Minh Duc Ly; Que Nguyen Kieu Viet. "Improvement Productivity and Quality by Using Lean Six Sigma: A Case Study in Mechanical Manufacturing". *International Research Journal on Advanced Science Hub*, 4, 11, 2022, 251-266. doi: 10.47392/irjash.2022.066

[55] Ragunath A; Poonam Syal. "Net Zero Energy Buildings Initiatives - A Review". *International Research Journal on Advanced Science Hub*, 4, 11, 2022, 267-271. doi: 10.47392/irjash.2022.067

[56] Suresh P; Justin Jayaraj K; Aravintha Prasad VC; Abishek Velavan; Mr Gokulnath. "Deep Learning for Covid-19 Identification: A Comparative Analysis". *International Research Journal on Advanced Science Hub*, 4, 11, 2022, 272-280. doi: 10.47392/irjash.2022.068

[57] Chirag H B; Darshan M; Rakesh M D; Priyanka D S; Manjunath Aradya. "Prediction of Concrete Compressive Strength Using Artificial Neural Network". *International Research Journal on Advanced Science Hub*, 4, 11, 2022, 281-287. doi: 10.47392/irjash.2022.069

[58] Minh Ly Duc; Que Nguyen Kieu Viet. "Analysis Affect Factors of Smart Meter A PLS-SEM Neural Network". *International Research Journal on Advanced Science Hub*, 4, 12, 2022, 288-301. doi: 10.47392/irjash.2022.071

[59] Lely Novia; Muhammad Basri Wello. "Analysis of Interpersonal Skill Learning Outcomes in Business English Students Class". *International Research Journal on Advanced Science Hub*, 4, 12, 2022, 302-305. doi: 10.47392/irjash.2022.072

DOI:10.46647/ijetms.2023.v07i02.052 ISSN: 2581-4621

[60] Ms. Nikita; Sandeep Kumar; Prabhakar Agarwal; Manisha Bharti. "Comparison of multi-class motor imagery classification methods for EEG signals". *International Research Journal on Advanced Science Hub*, 4, 12, 2022, 306-311. doi: 10.47392/irjash.2022.073
[61] Aniket Manash; Ratan Kumar; Rakesh Kumar; Pandey S C; Saurabh Kumar. "Elastic properties of ferrite nanomaterials: A compilation and a review". *International Research Journal on Advanced Science Hub*, 4, 12, 2022, 312-317. doi: 10.47392/irjash.2022.074
[62] Prabin Kumar; Rahul Kumar; Ragul Kumar; Vivek Rai; Aniket Manash. "A Review on coating of steel with nanocomposite for industrial applications". *International Research Journal on Advanced Science Hub*, 4, 12, 2022, 318-323. doi: 10.47392/irjash.2022.075
[63] Twinkle Beniwal; Vidhu K. Mathur. "Cloud Kitchens and its impact on the restaurant industry". International Research Journal on Advanced Science Hub, 4, 12, 2022, 324-335. doi: 10.47392/irjash.2022.076
[64] T. Pravin, C. Somu, R. Rajavel, M. Subramanian, P. Prince Reynold, Integrated Taguchi cum grey relational experimental analysis technique (GREAT) for optimization and material characterization of FSP surface composites on AA6061 aluminium alloys, Materials Today: Proceedings,Volume 33, Part 8, 2020, Pages 5156-5161, ISSN 2214-7853. doi.org/10.1016/j.matpr.2020.02.863.
[65] R. Ranjith, C. Somu, G. Tharanitharan, Venkatajalapathi.T, Naveenkumar M, Integrated Taguchi cum Grey Relational Experimental Analysis (GREAT) for Optimization and Machining Characterization of Cryogenic Cooled AA6063 Aluminium Alloys, Materials Today: Proceedings, Volume 18, Part 7, 2019,Pages 3597- 605, https://doi.org/10.1016/j.matpr.2019.07. 291.
[66] R. Devi Priya, R. Sivaraj, Ajith Abraham, T. Pravin, P. Sivasankar and N. Anitha. "Multi-Objective Particle Swarm Optimization Based Preprocessing of Multi-Class Extremely Imbalanced Datasets". International Journal of Uncertainty, Fuzziness and Knowledge-Based Systems Vol. 30, No. 05, pp. 735-755 (2022). Doi: 10.1142/S0218488522500209
[67] M. S. N. K. Nijamudeen, G. Muthuarasu, G. Gokulkumar, A. Nagarjunan, and T. Pravin, "Investigation on mechanical properties of aluminium with copper and silicon carbide using powder metallurgy technique," Advances in Natural and Applied Sciences, vol. 11, no. 4, pp. 277–280, 2017.
[68] Pravin T, M. Subramanian, R. Ranjith,Clarifying the phenomenon of Ultrasonic Assisted Electric discharge machining, "Journal of the Indian Chemical Society", Volume 99, Issue 10, 2022, 100705, ISSN 0019-4522, Doi: 10.1016/j.jics.2022.100705
[69] V.S. Rajashekhar; T. Pravin; K. Thiruppathi , "Control of a snake robot with 3R joint mechanism", International Journal of Mechanisms and Robotic Systems (IJMRS), Vol. 4, No. 3, 2018. Doi: 10.1504/IJMRS.2018.10017186
[70] T. Pravin, M. Sadhasivam, and S. Raghuraman, "Optimization of process parameters of Al-10% Cu compacts through powder metallurgy," Applied Mechanics and Materials, vol. 813-814, pp. 603–607, 2010.
[71] Rajashekhar, V., Pravin, T., Thiruppathi, K.: A review on droplet deposition manufacturing-a rapid prototyping technique. Int. J. Manuf. Technol. Manage. 33(5), 362–383 (2019) https://doi.org/10.1504/IJMTM.2019.103277
[72] Rajashekhar V S, Pravin T, Thirupathi K, Raghuraman S.Modeling and Simulation of Gravity based Zig-zag Material Handling System for Transferring Materials in Multi Floor Industries. Indian Journal of Science and Technology.2015 Sep, 8(22), pp.1-6.